A NEW TYPE CURVE ANALYSIS FOR SHALE GAS/OIL RESERVOIR PRODUCTION PERFORMANCE WITH DUAL POROSITY LINEAR SYSTEM

A Thesis

by

HAIDER JAFFAR ABDULAL

Submitted to the Office of Graduate Studies of
Texas A&M University
in partial fulfillment of the requirements for the degree of

MASTER OF SCIENCE

December 2011

Major Subject: Petroleum Engineering

A NEW TYPE CURVE ANALYSIS FOR SHALE GAS/OIL RESERVOIR PRODUCTION PERFORMANCE WITH DUAL POROSITY LINEAR SYSTEM

A Thesis

by

HAIDER JAFFAR ABDULAL

Submitted to the Office of Graduate Studies of
Texas A&M University
in partial fulfillment of the requirements for the degree of

MASTER OF SCIENCE

Approved by:

Chair of Committee,	Robert A. Wattenbarger
Committee Members,	Bryan Maggard
	Mahmoud El-Halwagi
Head of Department,	Steve Holditch

December 2011

Major Subject: Petroleum Engineering

ABSTRACT

A New Type Curve Analysis for Shale Gas/Oil Reservoir Production Performance with Dual Porosity Linear System. (December 2011)

Haider Jaffar Abdulal, B.S., University of Tulsa;

M.S., Texas A&M University

Chair of Advisory Committee: Dr. Robert Wattenbarger

With increase of interest in exploiting shale gas/oil reservoirs with multiple stage fractured horizontal wells, complexity of production analysis and reservoir description have also increased. Different methods and models were used throughout the years to analyze these wells, such as using analytical solutions and simulation techniques. The analytical methods are more popular because they are faster and more accurate. The main objective of this paper is to present and demonstrate type curves for production data analysis of shale gas/oil wells using a Dual Porosity model.

Production data of horizontally drilled shale gas/oil wells have been matched with developed type curves which vary with effective parameters. Once a good match is obtained, the well dual porosity parameters can be calculated. A computer program was developed for more simplified matching process and more accurate results. As an objective of this thesis, a type curve analytical method was presented with its application to field data. The results show a good match with the synthetic and field cases. The calculated parameters are close to those used on the synthetic models and field cases.

DEDICATION

I dedicate my work to my parents for their devoted support and encouragement throughout my life, and helping me to become the man I am today. I also dedicate my work to my wife, Fatima, for her patience and support during these years. I also want to dedicate my work to my daughter, Zahra, who gave me a reason to work hard as I can.

I also dedicate my work to my country, Saudi Arabia, for sponsoring and taking care of us through Saudi American Oil Company (ARAMCO).

I also dedicate my work to all my friends for their encouragement during my master's degree.

ACKNOWLEDGEMENTS

By the name of Allah, the most gracious the most merciful, all praises to him for his mercies and blessings that continue to guide and protect me through my life.

I want to express my sincere appreciation to my advisor, Dr. Robert A. Wattenbarger, for giving me the keys of his knowledge and patience, and for his contribution to this work. Dr. Wattenbarger spent his valuable time guiding and teaching me throughout my master's studies. He helped build and strengthen my bases of knowledge and showed me the way to excel in my future career. I am honored to work under such supervision and simple words cannot express my gratitude and appreciation to Dr. Wattenbarger.

I want acknowledge my committee members, Dr. Bryan Maggard and Dr. Mahmoud El-Halwagi, for accepting to be on my committee and for helping me produce this work.

I want to acknowledge all my professors along with the department head, Dr. Steve Holditch, at Texas A&M University for giving me some of the knowledge that made this work possible.

Finally, I want to acknowledge my friends and colleagues in the Reservoir Modeling Consortium; Anas Almarzooq, Ahmad Alkouh, Orkhan Samandarli, Ammar Agnia, Tan Tran, Hassan Al-Ahmadi, Hassan Hamam, Pahala Sinurat, Salman Mengal, Wahaj Khan, and Vartit Tivayanonda, for their support and friendship.

TABLE OF CONTENTS

CHAPTER Page

CHAPTER Page

LIST OF FIGURES

FIGURE Page

FIGURE Page

CHAPTER I

INTRODUCTION

Shale gas and shale oil are referred natural resources trapped within the shale formation. The important of these resources have increased with the advance of the technology in oil and gas industry all over the world. According to the Energy Information Administration, the production of shale gas increased from 1,293 Bscf to 3.110 Bscf within the last two years in the United States. This increase accounts to about ~ 15 % of total production. On the other hand the production of shale oil has tripled to about 275,000 BBL/Day within the period from 2005 to 2008 which accounts for ~ 3.5% of the total production. The production forecast of these resources is shows that they are going to play a major part of the energy supply in the next decade.

Shale gas/oil are considered unconventional resources because of the low permeability of the formation. Shale is a fine-grain sedimentary rock which acts as a sources rock and as a reservoir. These formations are usually very difficult to produce and disbursed on large quantities on very large areas.

The advancement on oil and gas technologies made the Shale gas/oil to economically viable. The real beginning was in the Barnett Shale in Texas where within one decade became the largest gas field in the state. The development started by drilling

This thesis follows the style of SPE Reservoir Evaluation & Engineering.

vertical wells until the advancement on horizontal drilling on the 2000. Then, these horizontal wells were stimulated with multistage hydraulic fracture. The success of the Barnett Shale attracted many investors and led to many discovery and developments that translated to thousands of wells drilled in the United State within the last decade.

The complexity of producing such reserves led to also a complexity on characterizing, simulating, and forecasting. The use of multistage hydraulic fracture was to enhance the effective permeability of the well by creating more conductive surface flow area. The shape, permeability, areal extent, storativity, and other parameters are unknowns or involve high level of uncertainty. Using transit dual porosity linear models type curves for analyzing the performance of the wells can give some idea about characteristic of such reservoirs and completion. It will also give an idea about their impact on the long term production performance and their ultimate recovery.

Many models have been proposed by different authors. The very first model was pseudo-steady state dual porosity model by (Warren and Root 1963). Then, the transient model was proposed by (Kazemi 1969) and (de Swaan O. 1976). The first decline curves for dual porosity radial system was proposed by (Da Prat 1981). Then, Hazlett (1986) developed constant pressure type curves for dual porosity system but they were specifically made for Devonian Shale.

1.1 Motivation

Motivation of this started by recent advancement on exploration and production of Shale gas/oil in all over the world. It is essential know about completion of your well

and its long term production performance that well impact any future development plans for the field. Subsequently, it will help for better economic planning for any future projects.

1.2 Objectives

The main objective of this paper is to present and demonstrate type curves for production data analysis of shale gas/oil wells using a Dual Porosity model. Dual Porosity model is based on (Bello and Wattenbarger 2010) mathematical model where hydraulic fractures act as a secondary porosity where matrix is the primary porosity. Samandarli (2011) showed application of this model on history matching and forecasting of shale gas wells with multiple fractures by doing regression on effective fracture permeability and half length. This type of regression is as rigorous as simulation, however much faster than it. On the other hand for "quick look interpretation" having type curves will make the production analysis even more convenient for practical purposes.

1.3 Organization of the Thesis

This thesis is divided into seven chapters. Organization of the thesis was developed in following way.

Chapter I is an introduction of thesis with objectives, motivation, and description of thesis parts.

In Chapter II, a brief description of literature review is outlined. Theoretical information is given about Dual Porosity models, linear flow in hydraulically fractured shale reservoirs, and type curve analysis of dual porosity reservoirs.

Chapter III gives information about linear Dual Porosity model with a brief description of model assumptions, definition of dimensionless variables, different regions, and important parameter group affecting different regions.

Chapter IV gives sensitivity of different dual porosity parameters and then discusses in depth the effect of the physical parameter of the linear dual porosity system.

Chapter V describe the creation of type curve for the dual porosity linear system accompanied with assumption, definition of dual porosity model effective parameters, parameters modification, field cases coverage, axis modification, and parameters calculations.

Chapter VI discusses type curve validation and application with some synthetic cases generated by GASSIM and CMG simulators. Then, it presents some field application with discussion of the results.

Chapter VII discusses conclusions and recommendations.

CHAPTER II

LITERATURE REVIEW

2.1 Dual Porosity Systems

The purpose of the Dual Porosity Model was originally to simplify the naturally fracture reservoirs. It is also can be used to model a reservoir with two different storage systems. Warren and Root (1963) showed that non-homogeneous reservoirs shown on Fig. 2.1 can be represented by two dimensionless parameters; lambda and omega. Lambda, the inter-porosity parameter, is related to the scale of heterogeneity that presents in the system and omega, the storativity parameter, is the measure of flow storativity of the secondary porosity system. In a dual porosity reservoir, the matrix will normally hold the primary porosity of the system and will not contribute to the flow capacity. On the other hand, the fracture system (hydraulic fracture) will not contribute much to the storage and will be treated as a secondary porosity system. Nevertheless, it will dominate the flow capacity of the system and will be the only medium to transmit the fluid.

Warren and Root (1963) showed the solution of such system by solving the continuity equation using Laplace Transformation proposed by (Everdingen and Hurst 1949). They assume Pseudo-steady station flow between the primary and secondary porosity.

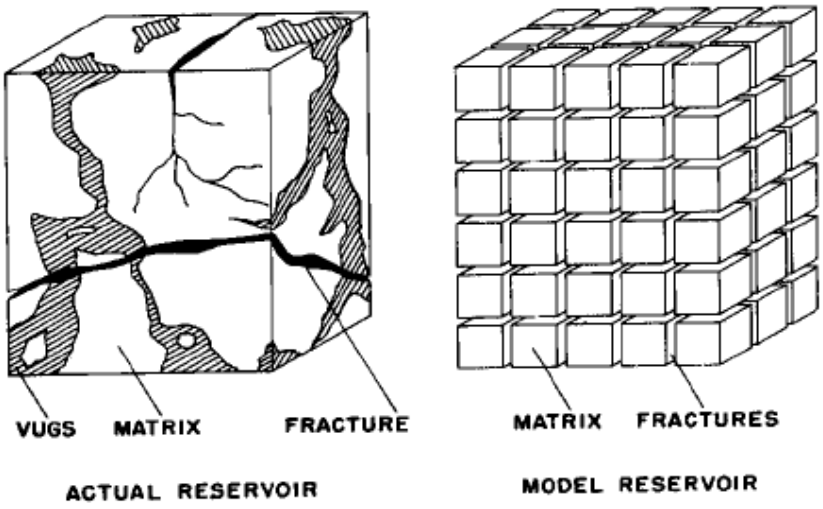

Fig. 2.1—Idealization of double porosity system with "sugar cube" model (Warren and Root 1963)

Kazemi (1969) proposed another approach assuming unsteady state flow in the matrix system as shown on Fig.2.2. This would decrease the error caused by incorrect pseudo steady state flow assumption for early time but it was no different that the results presented by (Warren and Root 1963). Fig 2.3 shows the difference was only in the transition period between the fracture system and the matrix system during the buildup or drawdown tests.

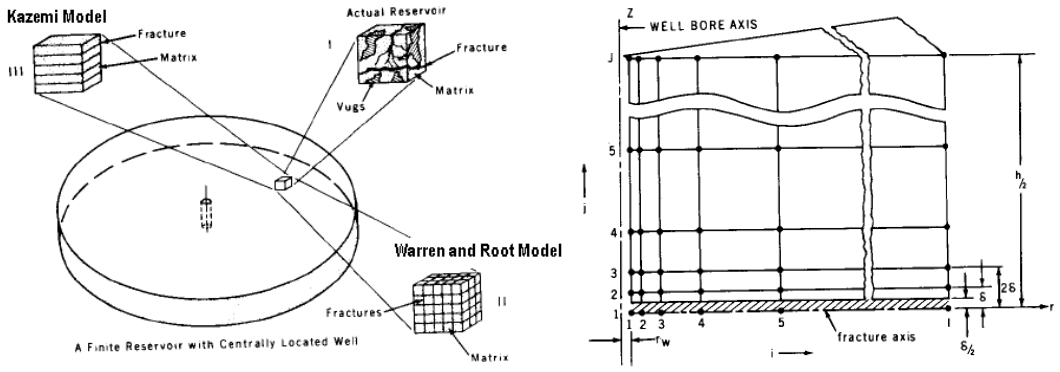

Fig. 2.2—Idealization of double porosity system with slabs (Kazemi 1969)

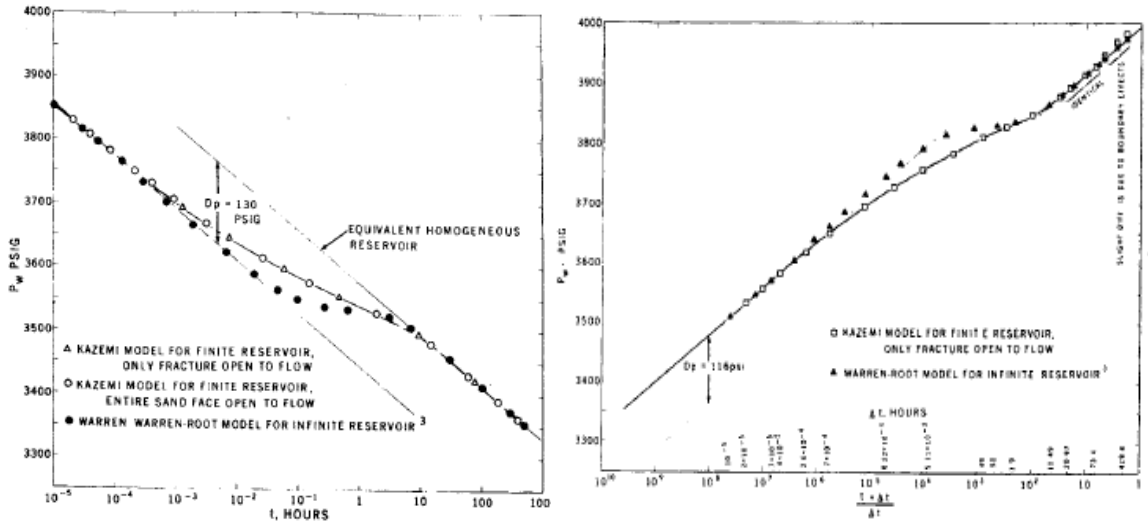

Fig. 2.3—Buildup and drawdown results comparison between Warren and Root dual porosity systems with slabs (Kazemi 1969)

Most other models used after (Warren and Root 1963) and (Kazemi 1969) were using their assumption for the fluid flow between the primary and secondary porosity systems.

2.2 Linear Flow in Hydraulically Fractured Reservoirs

Linear flow equations in dual porosity reservoirs were initially proposed by (El-Banbi 1998) in his dissertation. The analytical solutions in Laplace domain are given by

Constant rate case: $$\overline{P_{wDL}} = \frac{2\pi}{s\sqrt{sf(s)}}\left[\frac{1+\exp(-2\sqrt{sf(s)}y_{De}}{1-\exp(-2\sqrt{sf(s)}y_{De}}\right] \quad \text{..... (2.1)}$$

Constant rate case: $$\frac{1}{\overline{q_{DL}}} = \frac{2\pi s}{\sqrt{sf(s)}}\left[\frac{1+\exp(-2\sqrt{sf(s)}y_{De}}{1-\exp(-2\sqrt{sf(s)}y_{De}}\right] \quad \text{..... (2.2)}$$

Arevalo-Villagran (2001) showed that long term linear flow in tight reservoir might be caused by anisotropy, linear or elongated reservoirs, high permeability streaks, naturally fractured reservoirs, and hydraulic fractures. The norm in most of the development of Shale gas/oil in the United States is to drill a horizontal well stimulated with a multistage hydraulic fracture. These wells utilize the hydraulic fracture as their primary flow medium creating a linear flow effect. Depending on the type of completion, the matrix typically flows into the fracture only and the drainage area extend only to the extent of the hydraulic fracture. Bello and Wattenbarger (2008) proposed different methods and models to analyze hydraulically fracture shale wells. Their primary (Model-1) assumes that the hydraulic fracture is the only flow medium feeding the well in the system while the matrix will flow only to the hydraulic fracture. The system is considered a dual porosity system where the matrix will be a primary porosity and the fractures will be the secondary porosity of the system. Fig 2.4 shows a schematic of slab matrix linear model of hydraulically fractured well.

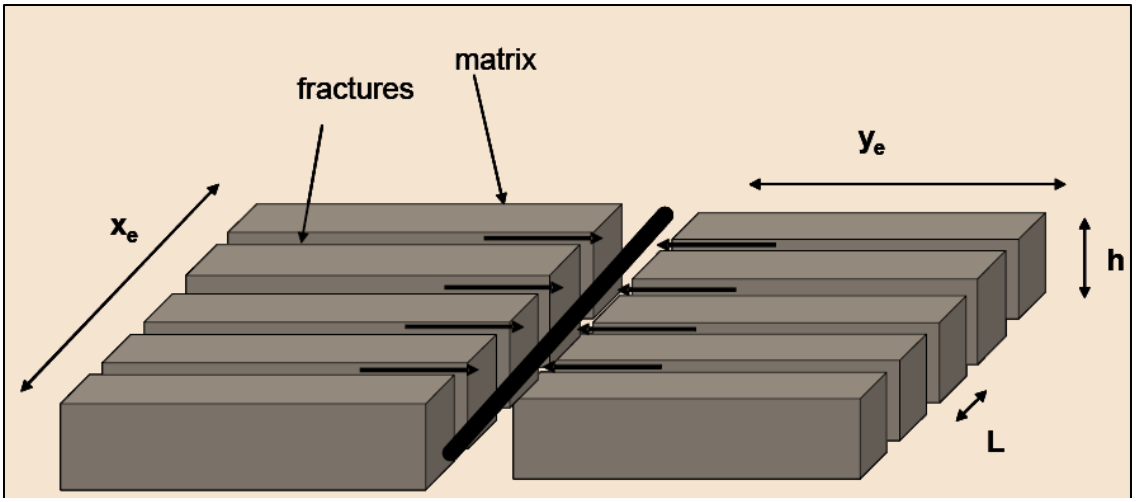

Fig. 2.4—Schematic of slab matrix linear model of hydraulically fractured well (Bello and Wattenbarger 2010)

2.3 Type Curve Analysis of Dual Porosity Reservoirs

Da Prat (1981) developed decline curves for dual porosity radial flow system. The system assumption was based on (Warren and Root 1963) model. The solution was in dimensionless form for constant pressure solution only. It lacks uniqueness and requires the use of almost 20 type curves. It is controlled by the two dual porosity parameters; lambda and omega and also the wellbore outer radius. They concluded that type curve matching for dual porosity is difficult when there is no prior knowledge of dual porosity parameters.

Hazlett (1986) developed constant pressure dual porosity type curves for Devonian Shale using unsteady-state analytical model. The characteristics observed from the different well performances were used to correlate and create a special production data analysis type curve for this Shale. The set of curves are in dimensionless

form and can be used only for constant pressure radial systems. The solution lacks uniqueness where many good matches can be found.

Linear flow equations in dual porosity reservoirs were initially proposed by (El-Banbi 1998) in his dissertation. Bello and Wattenbarger (2008) proposed a mathematical model for horizontal shale gas well stimulated with multiple hydraulic fractures. One important finding is that reservoir functions, *f(s)* which is derived for radial flow can be used in linear flow solutions in Laplace domain and vice versa.

Bello and Wattenbarger (2009) showed that El-Banbi solutions could be used in modeling horizontal well performance with multi-stage fractured for tight reservoirs for constant pressure solution.

Bello and Wattenbarger (2009) and (Bello and Wattenbarger 2008, 2009, 2010) utilized the dual porosity linear flow model in shale gas well performance analyze. Based on the constant pressure solution, five flow regions were defined. Region 4, where the transient linear flow from a homogeneous matrix, was used to effectively analyze the performance of Shale gas wells. A mathematical equation was suggested to account for skin effect that is affecting the early flow periods.

Moghadam (2010) generated dual porosity type curves for several values of lambda and omega. A workflow was proposed to evaluate reservoir properties such as effective permeability and areal extent of the fracture system. The workflow is lengthy and involves so many variables. They concluded that the analysis is meaningless if no good estimate of lambda or omega is available.

CHAPTER III

DESCRIPTION OF LINEAR DUAL POROSITY MODEL

3.1 Introduction

In this chapter important assumptions for linear Dual Porosity model are discussed briefly. The dimensionless variables are shown and a brief description of each flow region is given.

3.2 Model Assumptions

The Dual Porosity Model was presented by (Bello and Wattenbarger 2010) to simplify the nature and behavior of the flow in hydraulically fractured shale gas wells as illustrated by (Ahmadi 2010) on Fig. 3.1. The model can also be used with hydraulically fractured tight gas and shale oil wells where governing flow regime is transient liner flow and reservoir geometry is rectangle.

The Following are the assumptions of Linear Dual Porosity Model:

- The drainage area is a rectangular geometry governs by the length of the well and the extent of the fracture system. This area is a called the Stimulated Reservoir Volume (SRV).
- The SRV is perforated with hydraulic fractures that enhance the fluid flow in low permeability reservoirs.

- Reservoir consists of matrix blocks and hydraulic fractures (slab model).
- The perforated length or well length, xe is the same as the length of the reservoir.
- Fluid drains in one direction where the matrix blocks drain to the hydraulic fractures and the hydraulic fractures drain to the wellbore.
- The flow inside the matrix block will reach a no flow boundary defined by half of the fracture spacing, L_F.
- The Constant bottomhole flowing pressure and constant rate cases are solved by using the transient dual-porosity solutions proposed by (El-Banbi and Wattenbarger 1998).

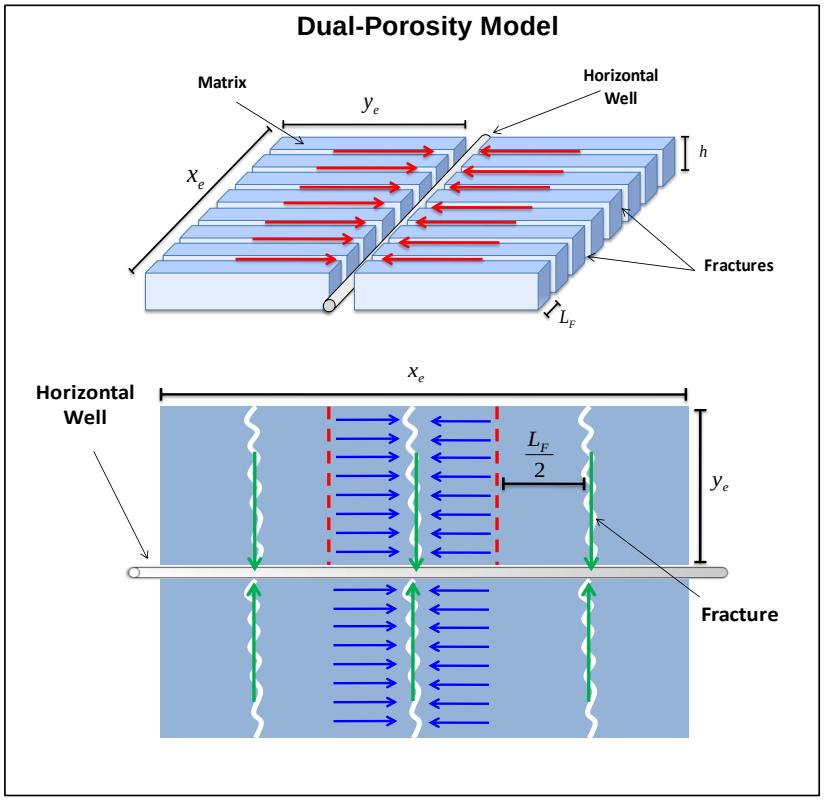

Fig. 3.1—Sketch for dual porosity model (Ahmadi 2010)

3.3 Definition of Dimensionless Variables

The following are the dimensionless variables for constant pressure solution and dual porosity parameters that is used for the linear dual porosity system.

$$t_{DA_{cw}} = \frac{0.00633 k_{effective} t}{\phi \mu c_t A_{cw}} \quad \text{..... (3.1)}$$

For gas: $$\frac{1}{q_{DL}} = \frac{k_{effective}\sqrt{A_{cw}}\left[m(p_i) - m(p_{wf})\right]}{1422 q_g T} \quad \text{..... (3.2)}$$

For oil: $$\frac{1}{q_{DL}} = \frac{k_{effective}\sqrt{A_{cw}}\left[p_i - p_{wf}\right]}{141.2 q_o B \mu} \quad \text{..... (3.3)}$$

$$\lambda_{Acw} = \sigma \frac{k_m}{k_{effective}} A_{cw} \quad \text{..... (3.4)}$$

$$\sigma = \frac{4n(n+2)}{L_F^2} \quad where \;\; n = 1,\ 2, or\ 3\ (n = 1\ \ for\ slab) \quad \text{..... (3.5)}$$

$$\omega = \frac{\left[\phi V c_t\right]_F}{\left[\phi V c_t\right]_t} \quad \text{..... (3.6)}$$

$$y_{eD} = \frac{y_e}{\sqrt{A_{cw}}} \quad \text{..... (3.7)}$$

$$A_{cw} = 2 x_e h \quad \text{..... (3.8)}$$

3.4 Description of Flow Regions

Bello and Wattenbarger (2010) observed five flow regions for the dual porosity model solution. Most of their work was on Region 4, which is the transient linear flow

from the matrix to the hydraulic fractures. This region is observed in all field data. The early flat region in the production performance plot is assumed to be the result of a skin effect which can be caused by linear flow convergence, completion, or production problems. Fig. 3.2 shows an illustration of the five flow regions for a slab matrix dual porosity linear reservoir.

Region 1 is the transient linear flow from hydraulic fractures to the wellbore. It is characterized by half slope on rate versus time log-log plot. Since the fracture have a higher permeability than the matrix and lower storage, the extent of this region is very short and it might not be observed in field data.

Region 2 is the transient bilinear flow where two transient linear flows occur at the same time. One of these transient linear flows occurs from the matrix to the hydraulic fractures whereas the other one occurs from the hydraulic fractures to well. It is characterized by quarter slope on rate versus time log-log plot. This region is observed in some of the field data such Fayetteville and Barnett.

Region 3 is the linear flow for homogenous system. This type of flow will be observed on the shale gas/oil that has not been fracture stimulated. Wells with this type will not flow at economical rates due to the low permeability of the shale.

Region 4 is the transient linear flow from the matrix to the hydraulic fracture. It is characterized by half slope on rate versus time log-log plot. This region is observed in all field data. Most of (Bello and Wattenbarger 2010) work was on this region.

Region 5 is the boundary dominated flow of the Fracture Stimulated Reservoir (SRV). It will happen at the end of the half slope of region 4. The curve will bend down on log-log plot of rate versus time.

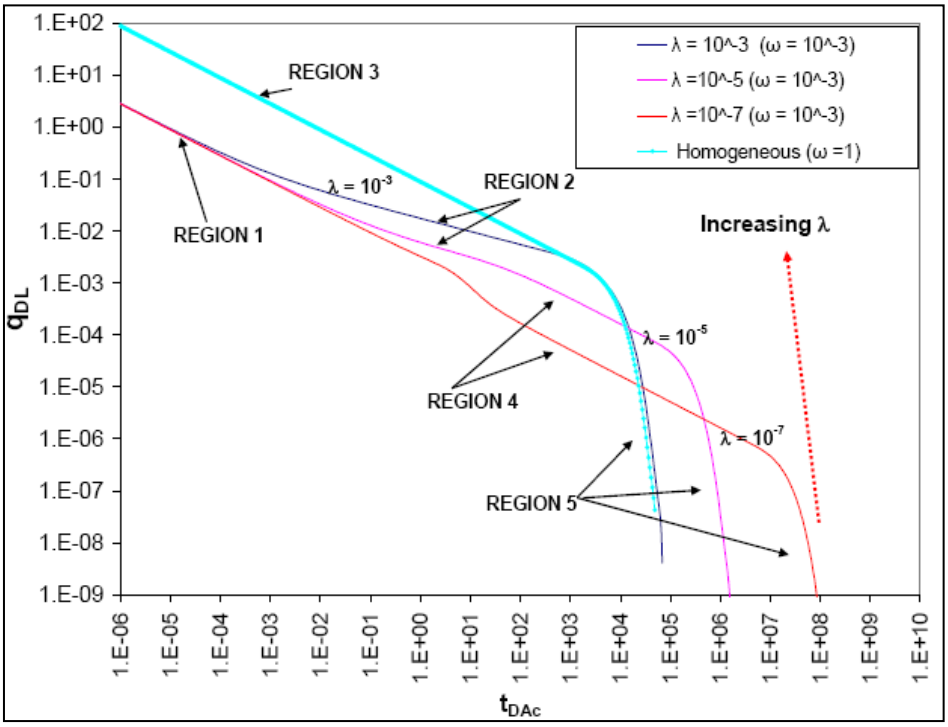

Fig. 3.2—Illustration of the five flow regions for a slab matrix dual porosity linear reservoir (y_{eD} = 100); λ_{Acw} =10^{-3}, 10^{-5}, 10^{-7} for values of ω = 10^{-3} (Bello and Wattenbarger 2010)

3.5 Chapter Summary

In this chapter, the key assumption and characteristics of Dual Porosity model proposed by Bello and Wattenbarger was discussed in detail. The dimensionless variables and solution were shown. Flow regions for Dual Porosity model were summarized.

CHAPTER IV

ANALYSIS OF LINEAR DUAL POROSITY SYSTEM PARAMETERS

4.1 Introduction

In this chapter the importance of dimensionless material balance time to the linear dual porosity system type curve will be discussed briefly. The effect of each dual porosity parameter on the shape of the curve on a rate versus time log-log plot will be shown. Furthermore, the effect of each physical parameter involved in calculating the dual porosity parameter will be shown briefly on rate versus time on a log-log plot.

4.2 Dimensionless Material Balance Time

Palacio and Blasingame (1993) were the first to propose a modern type curve method. He used pressure normalized rates and introduces the concept of material balance time. Material balance time or boundary-dominated superposition time is a method to convert constant pressure analytical solution to constant rate. It is a simple way to generate type curves with a single depletion stem regardless of the reservoir shape and size or drive mechanism. It will convert every decline in the production curve to negative slope stem for easier curve matching as illustrated on Fig 4.1. Material balance time for any time is the cumulative production divided by the rate at that time.

Following is (Palacio and Blasingame 1993) definition of the material balance time

$$t_{MB} = \frac{1}{q_g}\int_0^t qg\ dt = \frac{G_p}{q_g} \quad \text{..... (4.1)}$$

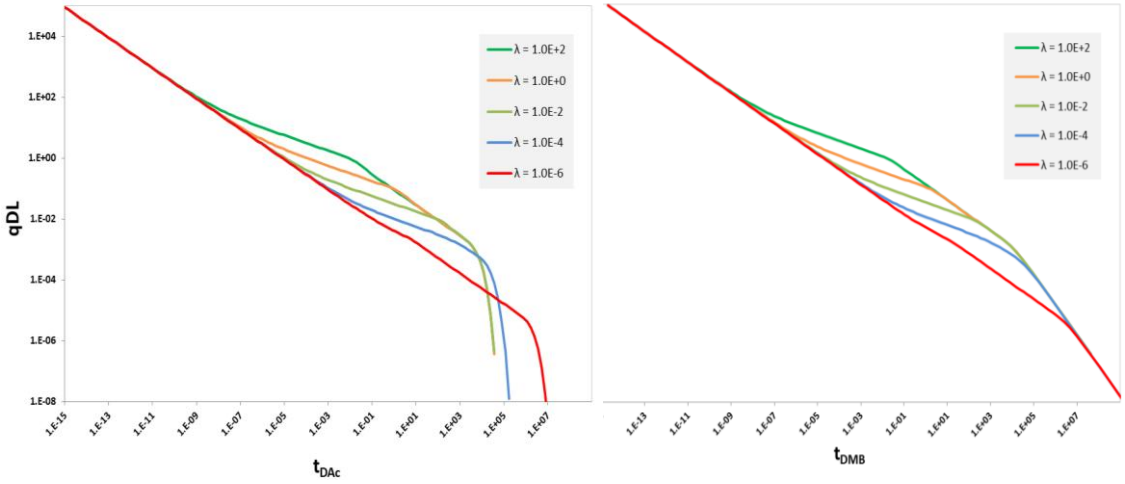

Fig. 4.1—Illustration of effect of material balance time on the shape of the well performance for different values of Lambda on log-log rate versus time plot

4.3 Dual Porosity Parameters Sensitivity

Different parameters of the dual porosity linear model will have different impact on the shape of the well performance curve. The main purpose of this sensitivity is to highlight the effect of these parameters on linear dual porosity model regions. The plots are generated using (El-Banbi 1998) solution and Stehfest algorithm to change the solution from the Laplace domain to the real domain.

Following are the important assumptions for these sensitivity runs

- The model used is the dual porosity transient-slab
- The flow is linear for constant pressure solution
- The outer reservoir boundary is for a closed system
- No skin or well storage effect

4.3.1 Effect of Dimensionless Fracture Half-Length

The dimensionless fracture half length is defined as the ratio of the fracture half length (y_e) to the square root of area of the well plane (A_{cw}). Fig 4.2 shows that the change in the dimensionless fracture half length value will affect the reservoir size which will change the time at which region 4 ends and the declining time. It will also lengthen all regions by as it increases. However, it will not affect the flow curves at beginning where all of them will start at the same stem. The change in dimensionless fracture half length only will not create a unique set of curves that will cover all cases of dual porosity linear model.

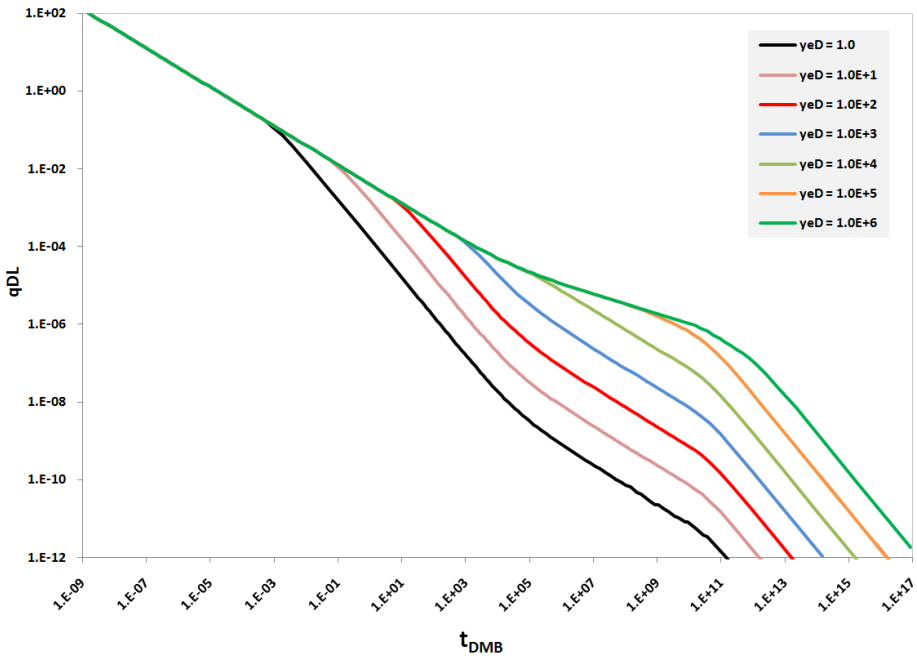

Fig. 4.2—Illustration of effect of fracture half length (y_{eD}) on the shape of the well performance on log-log rate versus time plot ($\omega = 10^{-3}$, $\lambda = 10^{-10}$)

4.3.2 Effect of Dimensionless Storativity Parameter

The dimensionless storativity ratio (Omega) is defined as the ratio of the fracture storativity to the storativity of the total system. Fig 4.3 shows that the change on the value of omega will change how the fractures dominate the flow which will be reflected on the length of region 1. Moreover, the length the transition between region 1 and 4 will increase as its value decrease. The flow curves will not start at same stem but they will all have the same decline stem. The change in dimensionless storativity ratio only will not create a unique set of curves that will cover all cases of dual porosity linear model.

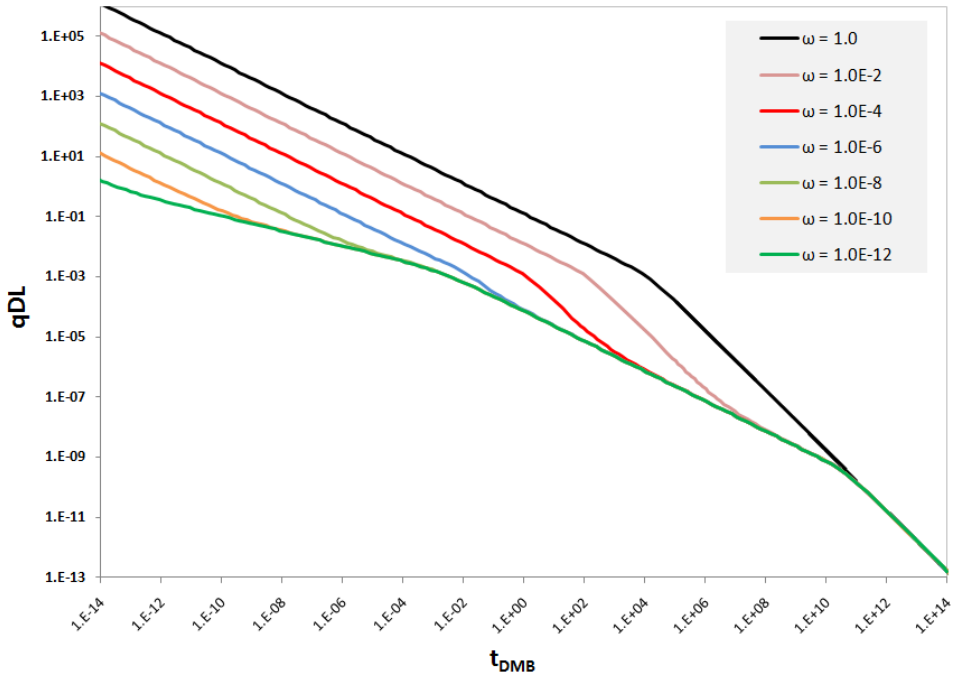

Fig. 4.3—Illustration of effect of storativity parameter on the shape of the well performance on log-log rate versus time plot (y_{eD} = 100, $\lambda = 10^{-10}$)

4.3.3 Effect of Dimensionless Inter-porosity Parameter

The inter-porosity parameter (Lambda) is defined as the ratio of the matrix permeability to the effective permeability multiplied by the shape factor and the area of well plane. Fig 4.4 shows that it controls whether the bilinear region 2 with its quarter slope will appears or not on the flow curve. If lambda value is low, the fractures flow will dominate the total flow which will make region 1 longer. On the other hand, if lambda value is high, the curve will turn up creating a bilinear flow with quarter slope. Furthermore, it makes the well deplete faster because the production will be higher throughout its life. The flow curves will start at same stem and at the same decline stem.

The change in dimensionless inter-porosity parameter only will not create a unique set of curves that will cover all cases of dual porosity linear model.

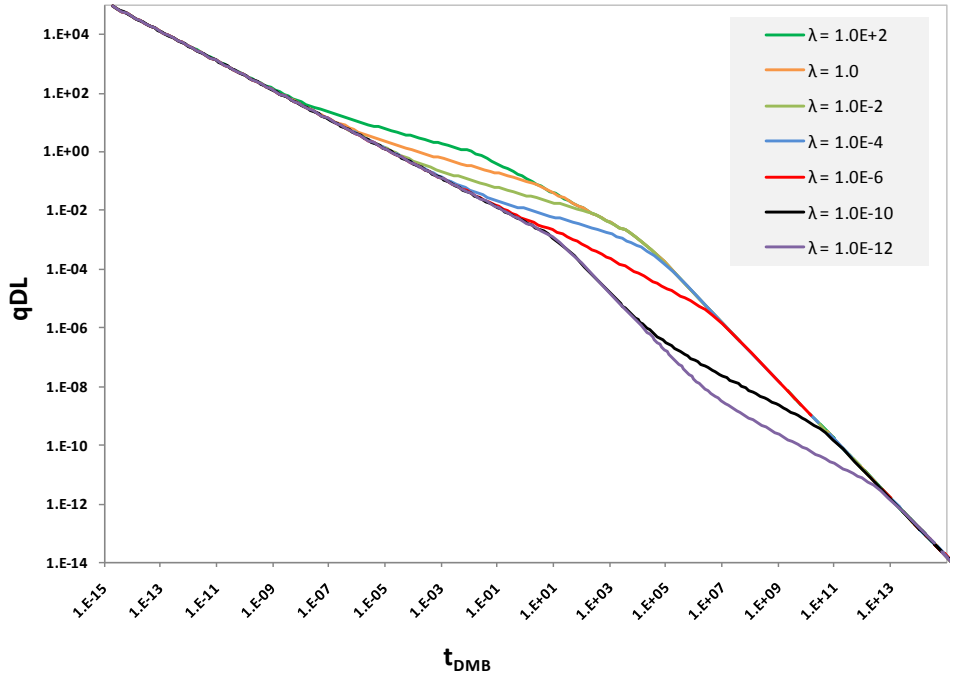

Fig. 4.4—Illustration of effect of inter-porosity parameter (λ) on the shape of the well performance on log-log rate versus time plot (y_{eD} = 100, ω = 0.001)

4.3.4 Effect of Group of Parameters

The change in one parameter did not create a unique set of curve that covers all flow types of linear dual porosity model. In this part, a sensitivity analysis is made to check the effect of changing group of parameters on the shape of the flow curves. The main purpose is to observe a trend or a behavior to will be utilized in simplifying the problem. The values of the dual porosity parameters were chosen randomly.

Figs. 4.5 and 4.6 illustrate the change of a group of parameters. The flow curves do not have a clear trend or behavior. Unlike what is observed when changing one variable, the curves are overlapping which creates a much difficult problem. Changing variables using this method was abandoned due to the lack of uniqueness.

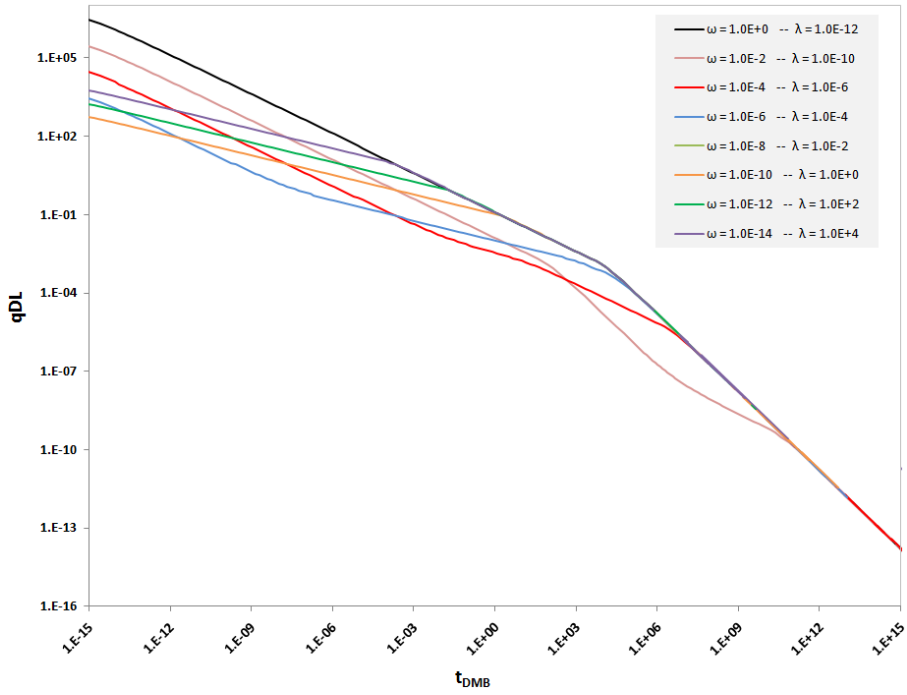

Fig. 4.5—Illustration of effect of inter-porosity parameter (λ) and storativity ratio (ω) on the shape of the well performance on log-log rate versus time plot (y_{eD} = 100)

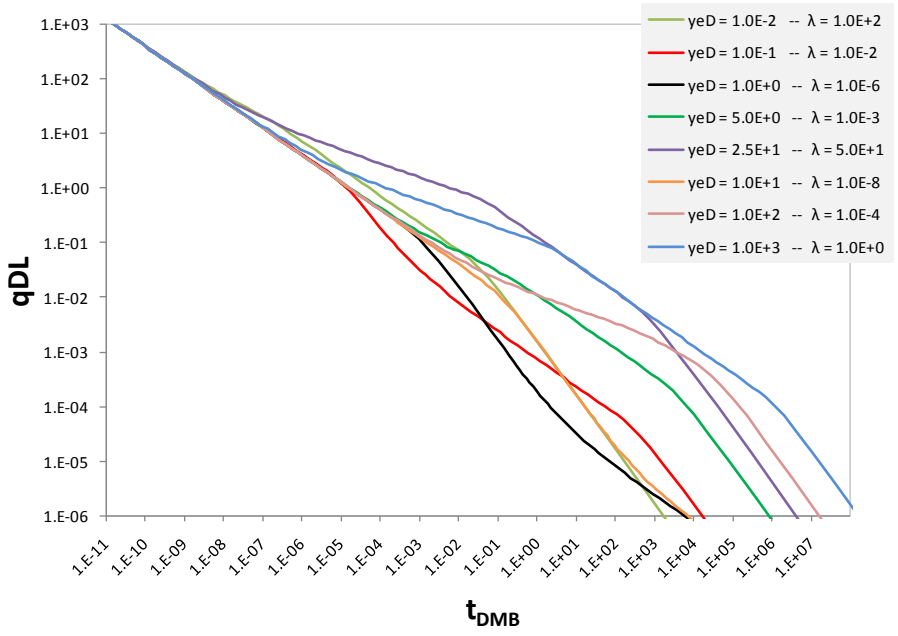

Fig. 4.6—Illustration of effect of inter-porosity parameter (λ) and dimensionless fracture-half length (y_{eD}) on the shape of the well performance on log-log rate versus time plot (ω = 0.001)

4.4 Physical Parameters Sensitivity

The change in dual porosity dimensionless parameters directly did not help in creating a unique set of type curves for the linear dual porosity model. To help clarifying the problem, these parameters were examined by examining their physical parameters involved the calculation. The purpose for this sensitivity defines the important set of parameters that should be involved on the creation of these type curves. Then, these parameters will be simplified or eliminated to overcome the problem of uniqueness.

4.4.1 Effect of Hydraulic Fracture Inner Permeability

Fig. 4.7 shows that any change on the hydraulic fracture permeability will impact all flow regions of the linear dual porosity model. This change is important because it will affect the flow of region 2, 4, and 5. Almost all the data of shale wells will have these regions as stated by (Bello and Wattenbarger 2010).

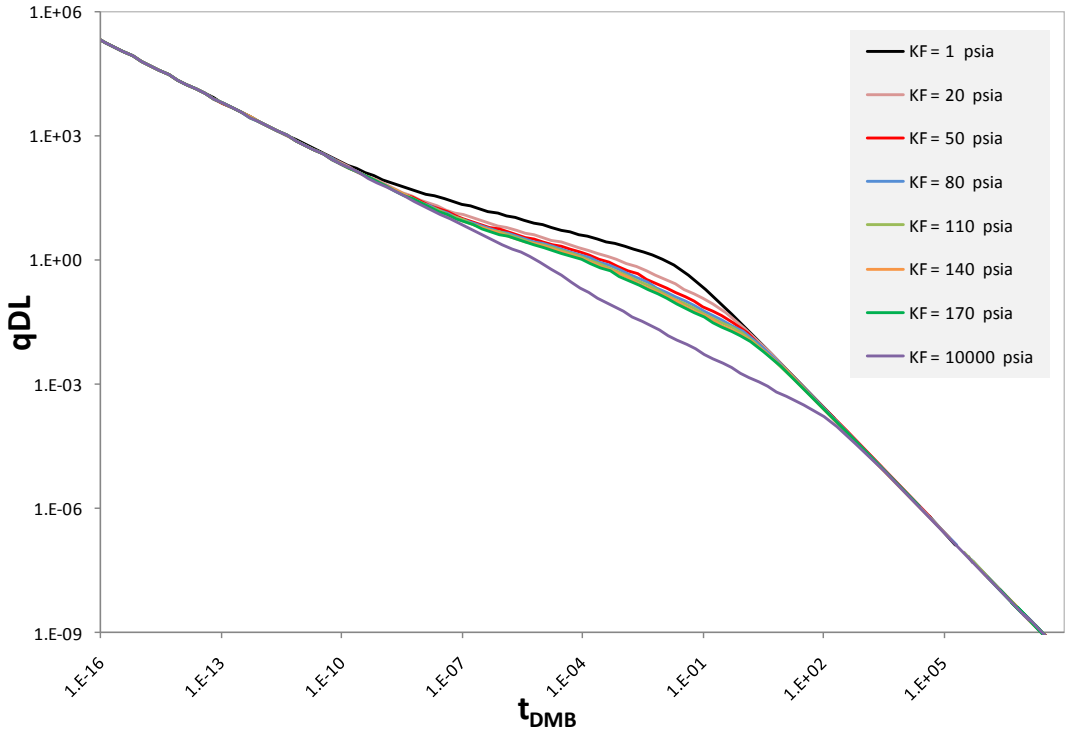

Fig. 4.7—Illustration of effect of hydraulic fracture inner permeability (k_F) on the shape of the well performance on log-log rate versus time plot

4.4.2 Effect of Hydraulic Fracture Inner Porosity

Hydraulic fracture inner porosity will change flow region 1 greatly as shown in Fig 4.8. This change is due to the change in the storativity ratio (ω). However, there is

no change on the other flow regions. This parameter can serve as one of the simplification because region 1 will appear only on the first flow few hours of the well life.

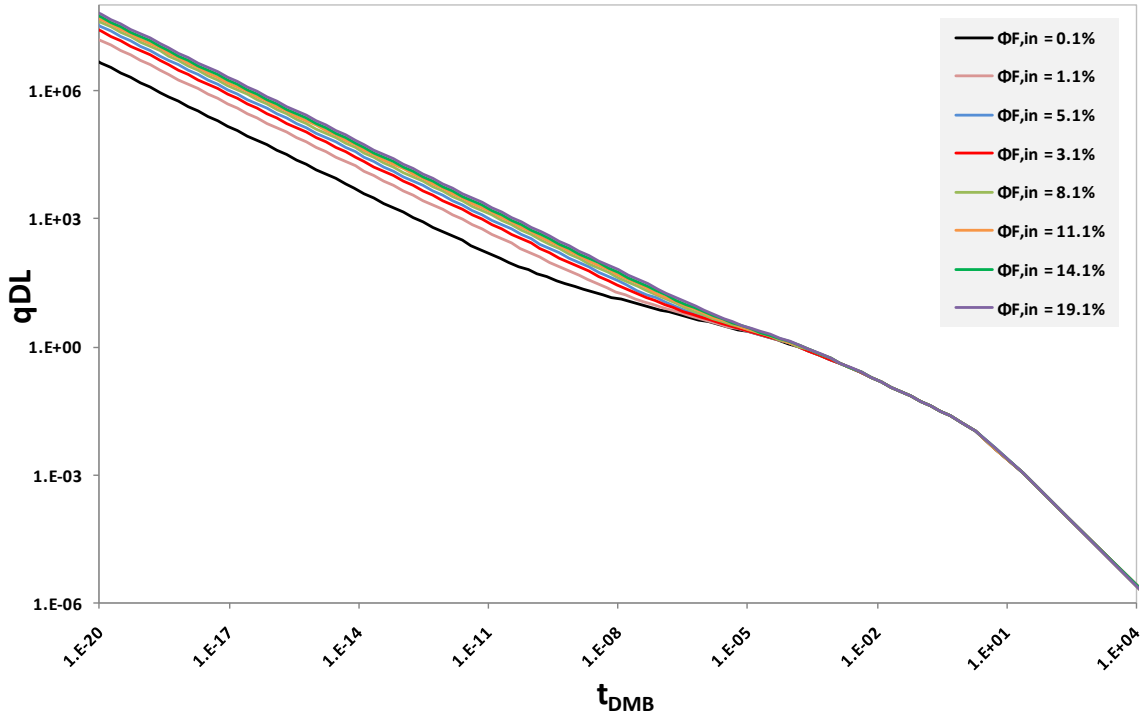

Fig. 4.8—Illustration of effect of hydraulic fracture inner porosity (ϕ_F) on the shape of the well performance on log-log rate versus time plot

4.4.3 Effect of Hydraulic Fracture Width

The hydraulic fracture width (w_F) will change the whole shape of the flow curves because it one of the parameters involved on both lambda and omega as shown on Fig. 4.9. It is one of the important parameters that should be considered greatly.

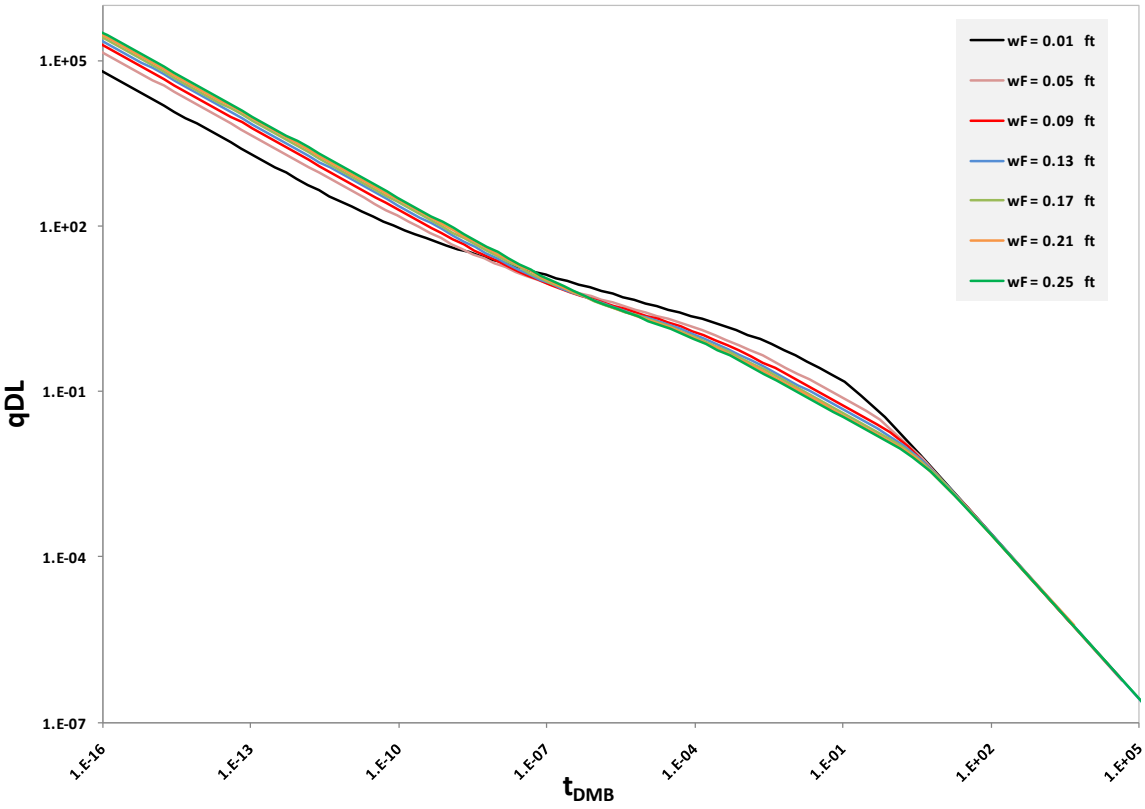

Fig. 4.9—Illustration of effect of hydraulic fracture width (w_F) on the shape of the well performance on log-log rate versus time plot

4.4.4 Effect of Hydraulic Fracture Spacing

The hydraulic fracture spacing will shift the flow curve diagonally as illustrated on Fig 4.10. Its impact is minimal if the curves are grouped together by modifying the X-axis and Y-axis which will be explained in later chapters. It can be consider as one of the simplification for the problem.

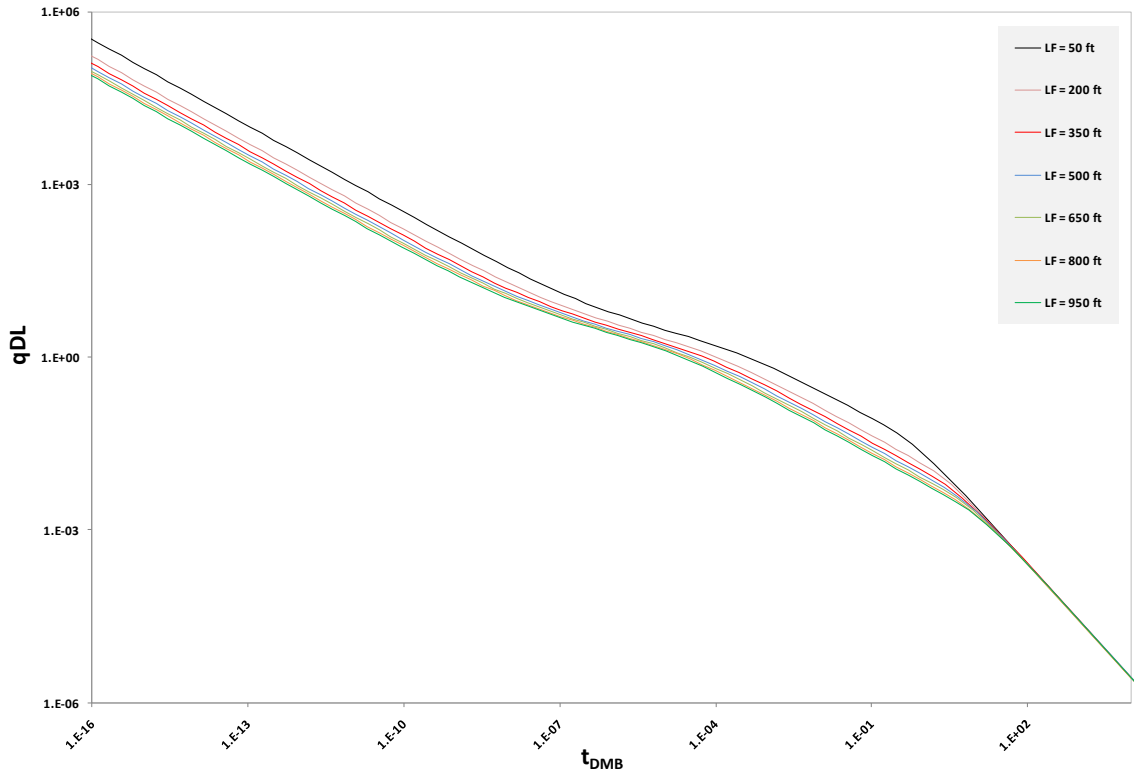

Fig. 4.10—Illustration of effect of hydraulic fracture spacing (L_F) on the shape of the well performance on a log-log rate versus time plot

4.4.5 Effect of Matrix Porosity

The effect of matrix porosity appears clearly on the beginning of the flow curves as shown in Fig. 4.11. It is involved in the calculation of the dual porosity parameter omega which greatly effect on region 1. On the other hand, it has a small or no effect on region 4 and 5. The flow curves will start at different stems and decline at the same stem.

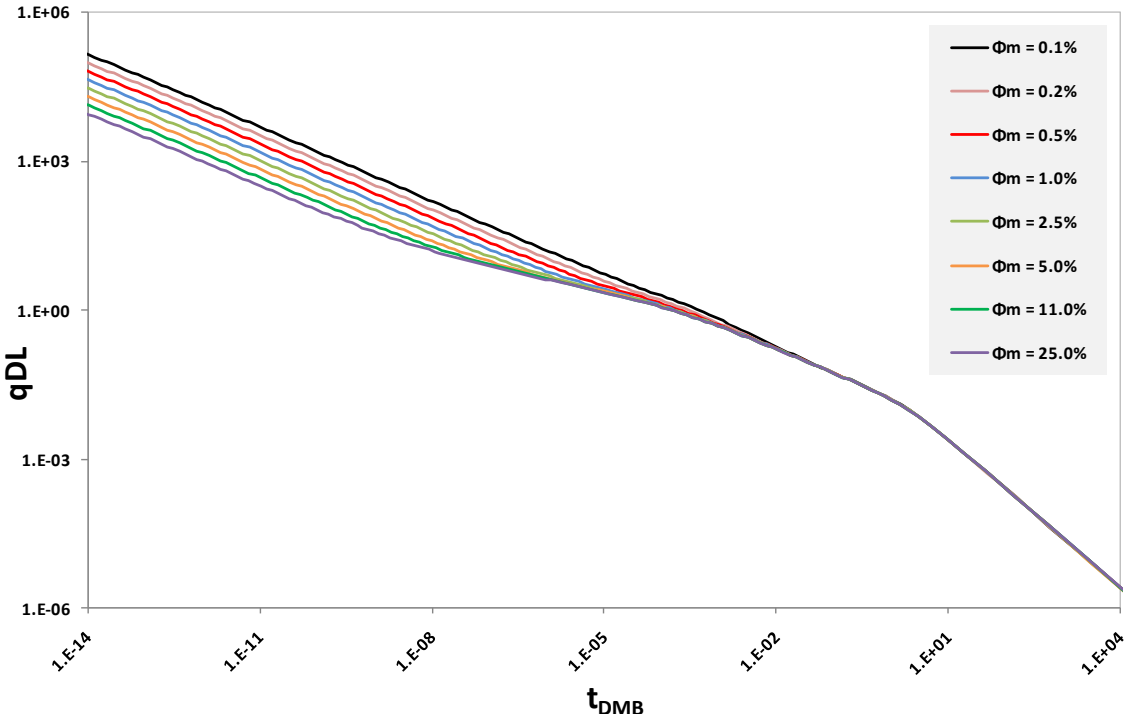

Fig. 4.11—Illustration of effect of matrix porosity (ϕ_m) on the shape of the well performance on log-log rate versus time plot

4.4.6 Effect of Matrix Permeability

The matrix permeability is one of important factors that define the shape of the type curves. It will affect all flow regions with the exception of region 1. It will also control whether the well has bilinear flow. As matrix permeability gets smaller the probability of having bilinear flow goes down as demonstrated on Fig. 4.12.

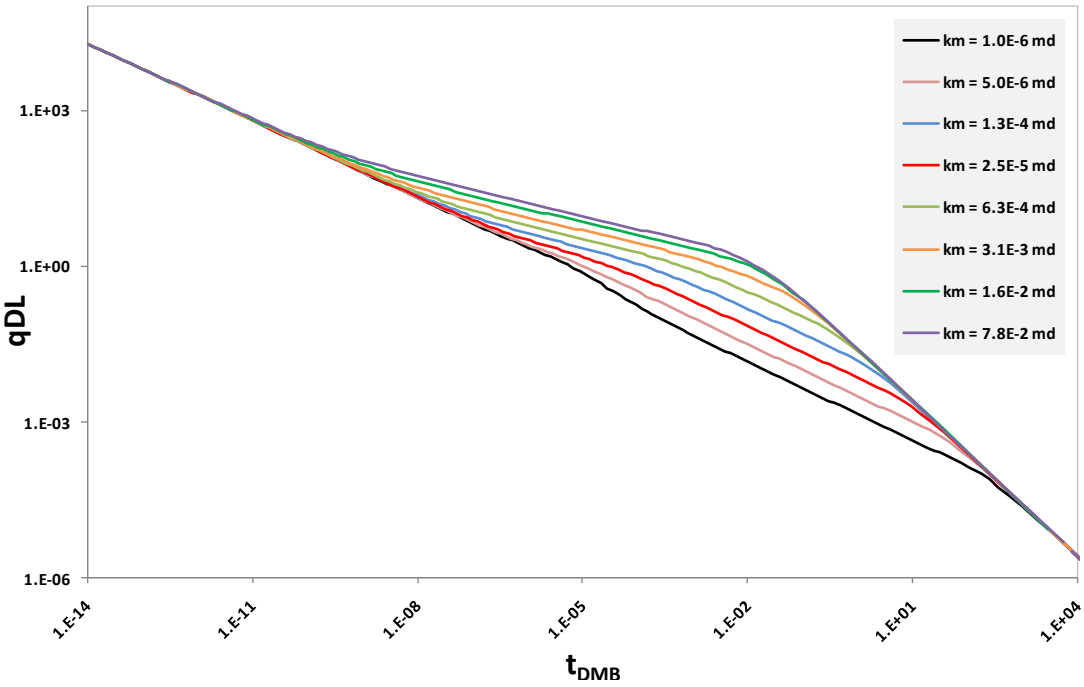

Fig. 4.12—Illustration of effect of matrix permeability (k_m) on the shape of the well performance on log-log rate versus time plot

4.4.7 Effect of Matrix Thickness

Matrix thickness will have a small effect on the shape of the flow curves. The flow regions are not affected with exception of region 5 as illustrated on Fig. 4.13. The transition between region 1 and 4 will have a small shift with a big change of the matrix thickness value. It can be considered as one of simplification parameters for this problem.

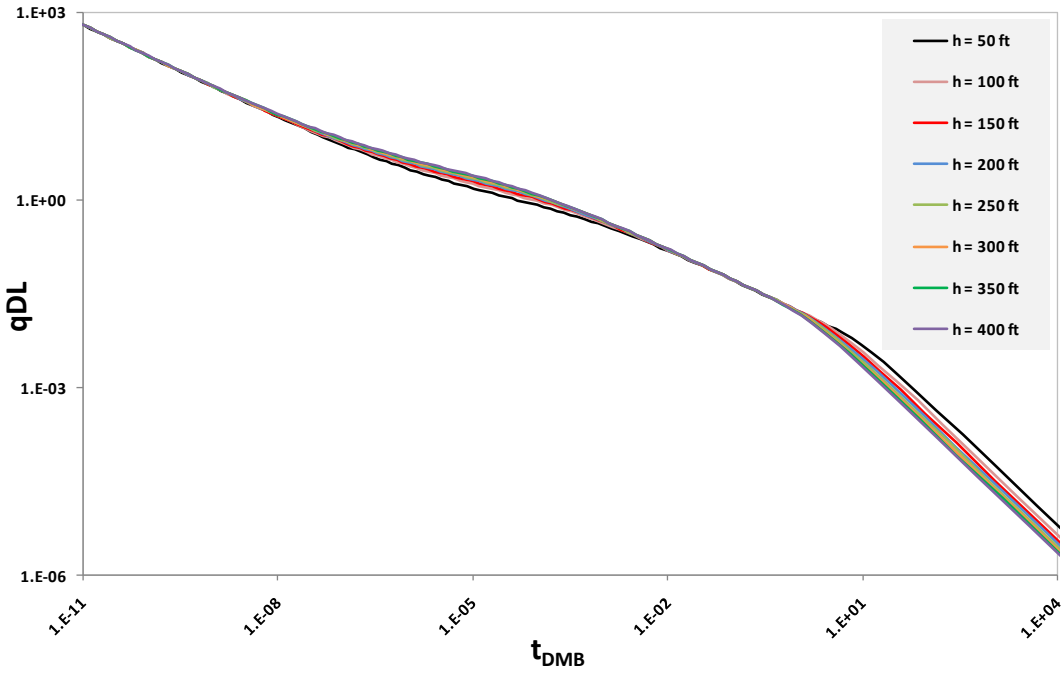

Fig. 4.13—Illustration of effect of matrix thickness (*h*) on the shape of the well performance on log-log rate versus time plot

4.5 Chapter Summary

In this chapter, different sensitivity runs were made for dual porosity and physical parameters with the implementation of material balance time. The change in one or more dual porosity parameters will not help in achieving a unique set of curves. The physical parameters sensitivity runs showed some important parameters and others that can be simplified or eliminated.

CHAPTER V

TYPE CURVE ANALYSIS FOR LINEAR DUAL POROSITY SYSTEM

5.1 Introduction

In this chapter, the effective parameters will be discussed briefly. Then, a detailed description and discussion of dual porosity parameters modification and assumption will be shown. A new type curve for linear dual porosity model will be illustrated with its field cases coverage, axis modification, derivation, match points, and calculation.

5.2 Definition of Dual Porosity Model Effective Parameters

The following are the effective dimensionless variables for dual porosity model that will be used on creating the type curve

$$\lambda_{Acw} = \sigma \frac{k_m}{k_{effective}} A_{cw} \quad \text{..... (5.1)}$$

$$\sigma = \frac{4n(n+2)}{L_F^2} \quad where \;\; n = 1,\ 2, or\ 3\ (n = 1\ \ for\ slab) \quad \text{..... (5.2)}$$

$$\omega = \frac{\left[\phi V c_t\right]_F}{\left[\phi V c_t\right]_t} \quad \text{..... (5.3)}$$

$$y_{eD} = \frac{y_e}{\sqrt{A_{cw}}} \quad \text{..... (5.4)}$$

5.3 Dual Porosity Model Parameters Modification and Assumptions

The effective parameters can be used to create a unique set of type curves. However, there are two limitations when using them directly. First, there are too many parameters to consider. Second, these parameters are not linked together mathematically. To overcome these limitations, some assumptions were made for some effective parameters while the others were modified to fit our objective.

Following are the assumption made for simplification:

- Matrix permeability (k_m), fracture spacing (L_F), well perforated length (x_e), and reservoir thickness are known
- Only linear constant pressure solution is used
- Reservoir has an infinite boundary
- The model used is the dual porosity transient-slab
- No skin or well storage effect
- The total compressibility of the fracture and total compressibility of the system are the same.

The known parameters are going to be used on the final calculation and going to be considered constant when creating type curves. The linear constant pressure solution is used because most of the wells have the same behavior.

The other limitation that prevents creating a unique set of type curves is the link between the effective parameters. When changing one of the dual porosity parameters, it should influence the other parameters as well. To achieve that, the effective parameters have been modified to be linked by a group of variables.

Following is the final modification made for the effective parameters

$$k_{effective} = \frac{k_m L_F + k_F w_F}{L_F + w_F} \quad \text{..... (5.5)}$$

$$\phi_{effective} = \frac{\phi_m L_F + \phi_F w_F}{L_F + w_F} \quad \text{..... (5.6)}$$

$$\omega_F^{'} = \frac{w_F \phi_F}{w_F \phi_F + L_F \phi_m} \quad \text{..... (5.7)}$$

$$\omega_F^{'} = \frac{1}{1 + \frac{\phi_m}{\phi_F}\left[\frac{(k_{effective} - k_F)}{(k_m - k_{effective})}\right]} \quad \text{..... (5.8)}$$

Refer to Appendix A for detailed modification.

5.4 Linear Dual Porosity System Type Curve

The modification in the effective dual porosity parameters links the parameters by effective permeability of the hydraulic fracture ($k_{effective}$). Fig. 5.1 demonstrate the change in the effective permeability will insure a change in the matrix permeability, fracture inner permeability, fracture spacing, and fracture width. The fracture porosity and matrix porosity are assumed to be constant for simplification because their effect

acts on region 1 only. Note that the dual porosity parameters Lambda (λ) and the dimensionless fracture half-length (y_{eD}). Lambda is already linked to the effective hydraulic fracture permeability while the dimensionless fracture half-length is going to be normalized using axis modification which will be explained in later chapters.

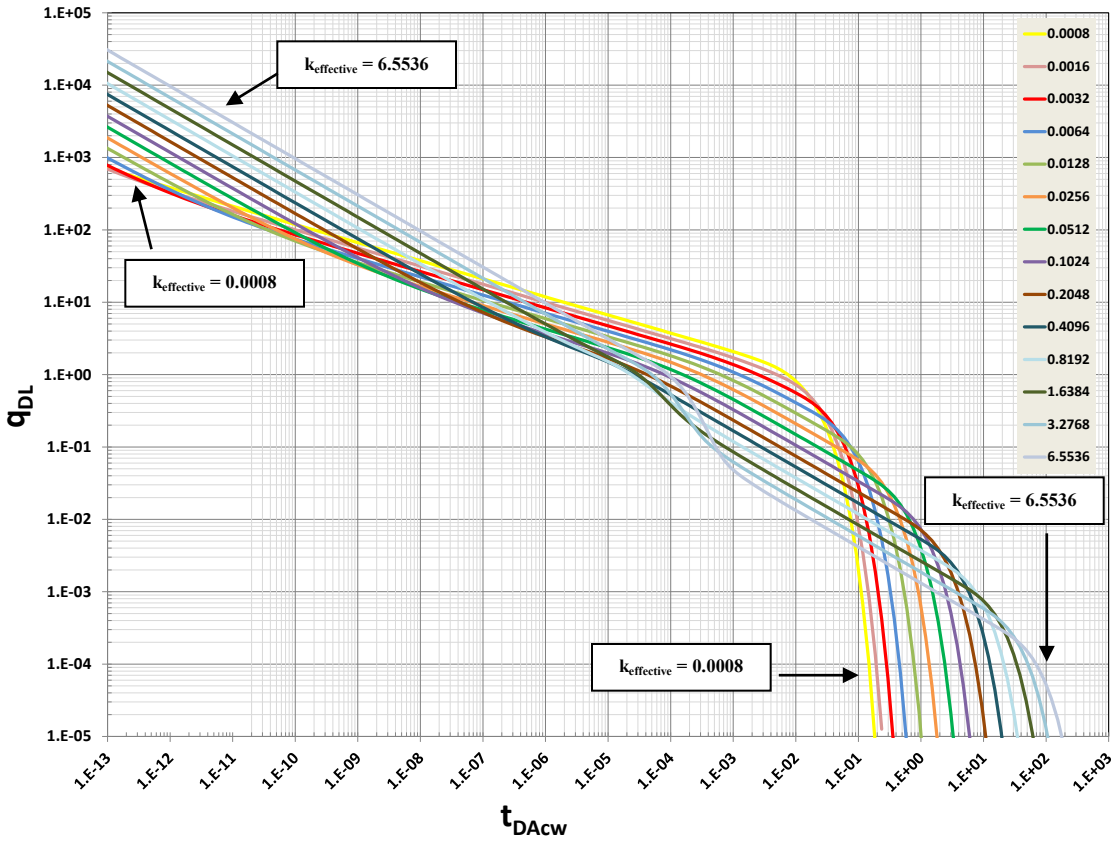

Fig. 5.1—Illustration of effect of modified effective parameters on the shape of the well performance on log-log rate versus time plot

5.4.1 Field Cases Coverage

The final type curve plot is shown in Fig. 5.1. This plot covers all well types observed on the field. Some curves start with half-slope and end up with another half-slope before start declining. Other curves start with half-slope and then go into a quarter-slope before going into another half-slope. Finally, some curves will start with half-slope and go into quarter-slope before declining. Figs. 5.2, 5.3, and 5.4 show an illustration of this coverage.

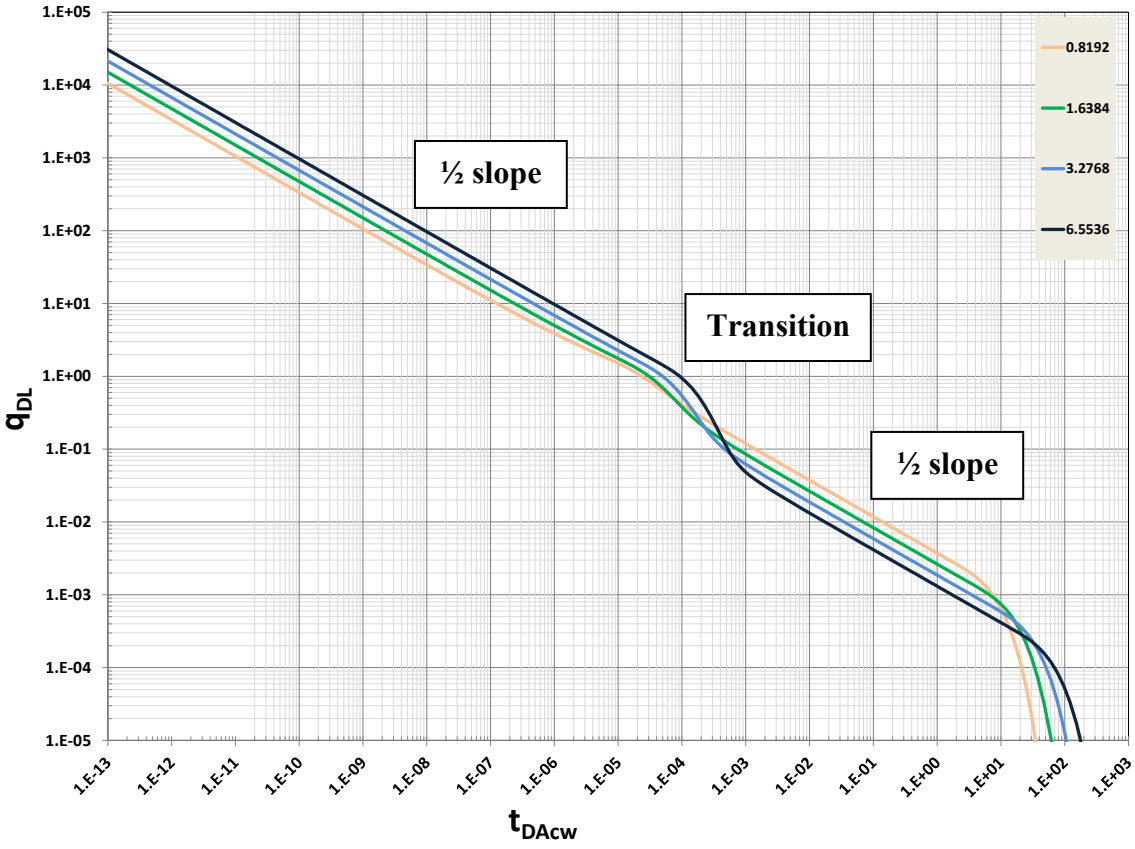

Fig. 5.2—Illustration of the coverage of the modified effective parameters for half-slope to half-slope on log-log rate versus time plot

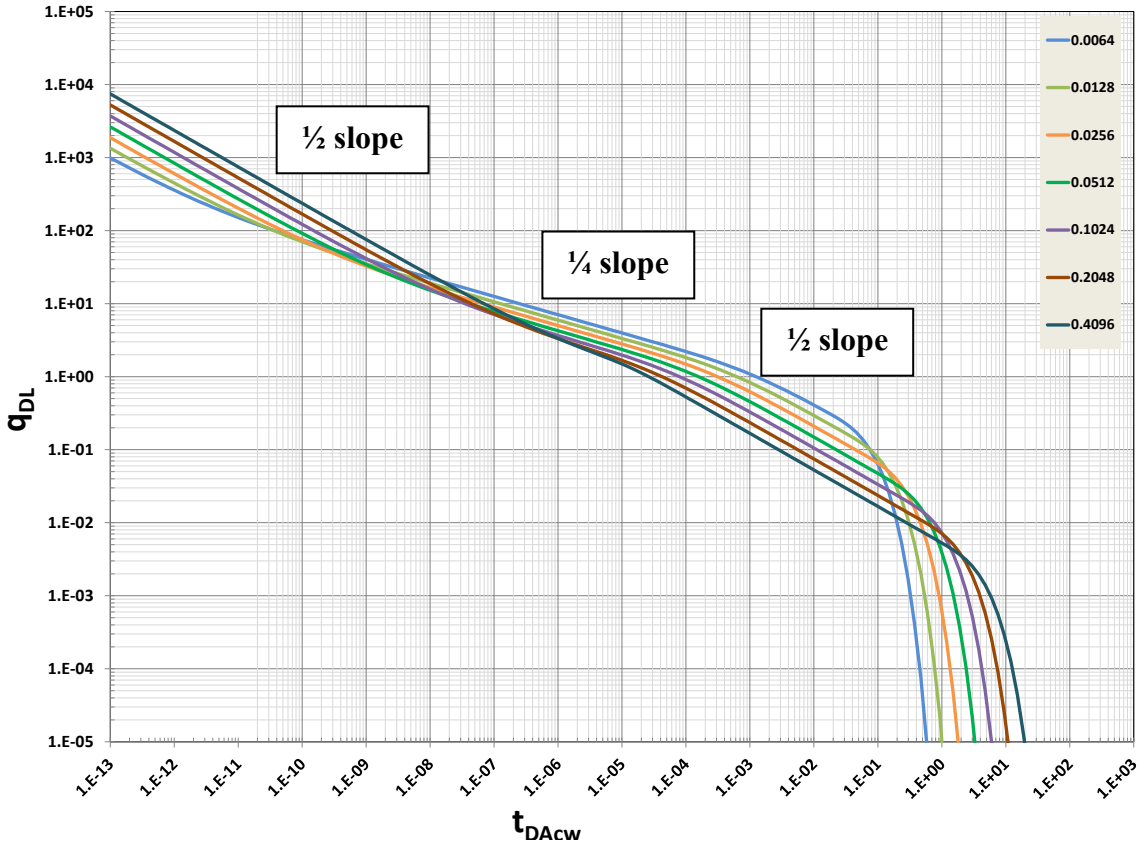

Fig. 5.3—Illustration of the coverage of the modified effective parameters for half-slope then a quarter-slope to another half-slope on log-log rate versus time plot

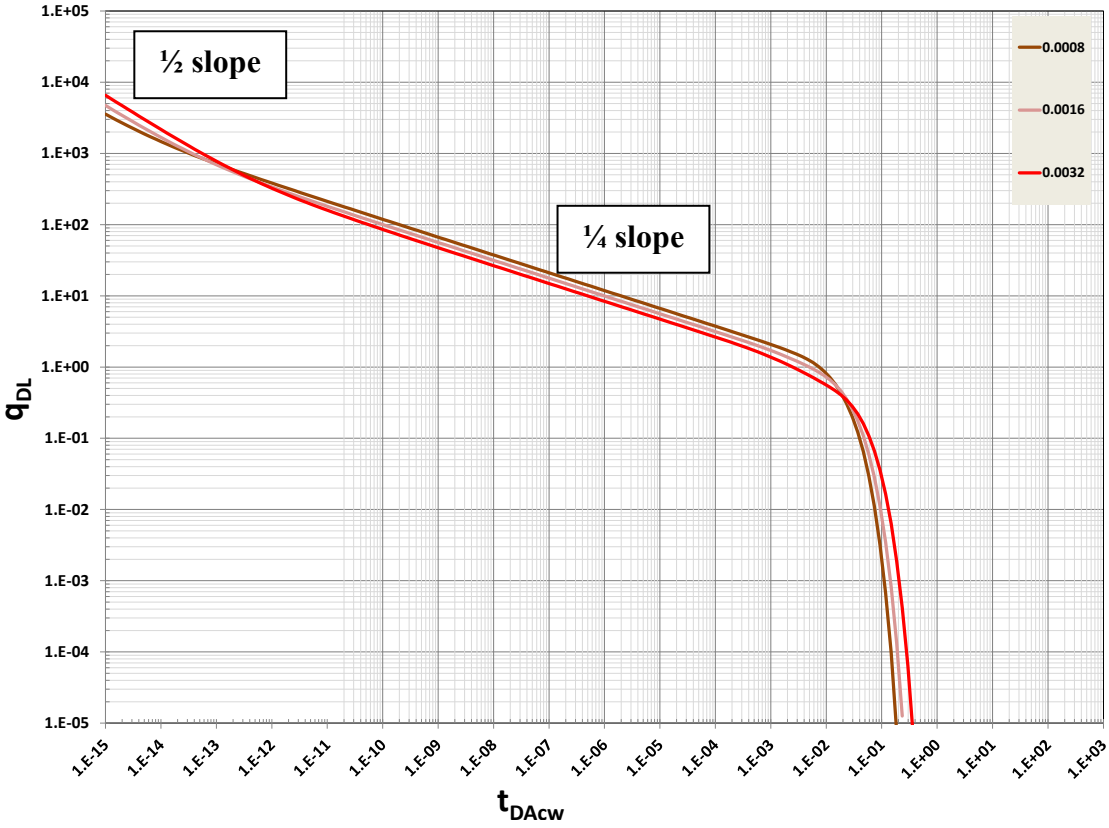

Fig. 5.4—Illustration of the coverage of the modified effective parameters for half-slope to quarter-slope on log-log rate versus time plot

5.4.2 Axis Modification

The axis for the final type curve plot has been modified for three reasons. First, it will make the curve fitting easier for the end user. Secondly, it will help in the final dual porosity and reservoir parameters calculation. Finally, it will normalize the effect of dimensionless fracture half-length.

The dimensionless fracture half-length (y_{eD}) was not linked to the modified parameters. Fitting the curves without any modification will result on a wrong reservoir size. Fig. 5.5 shows the effect of the dimensionless fracture half-length without

modification. The curves start at the same stem in region 1 but then have different stems for region 4 and 5.

To normalize the axis for this modification, the Y-axis is divided by the dimensionless fracture half-length. The curves are shifted and they all have one stem for region 4 and 5 as shown on Fig. 5.6. This is modification is going to be applied for the final type curves.

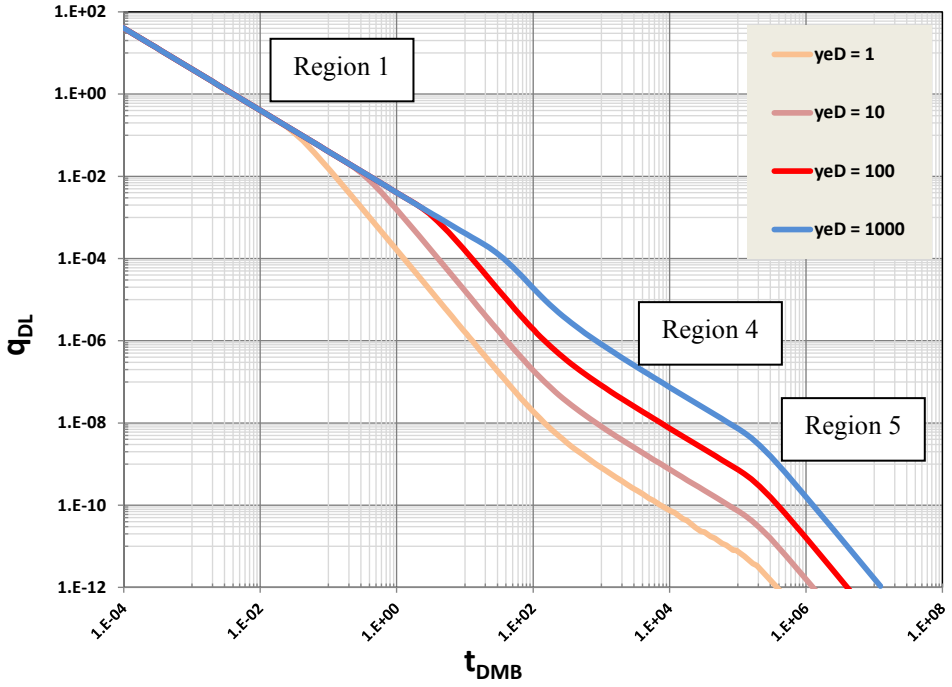

Fig. 5.5—Illustration of the effect of dimensionless fracture half-length without axis modification for a constant value of lambda and omega on log-log rate versus time plot

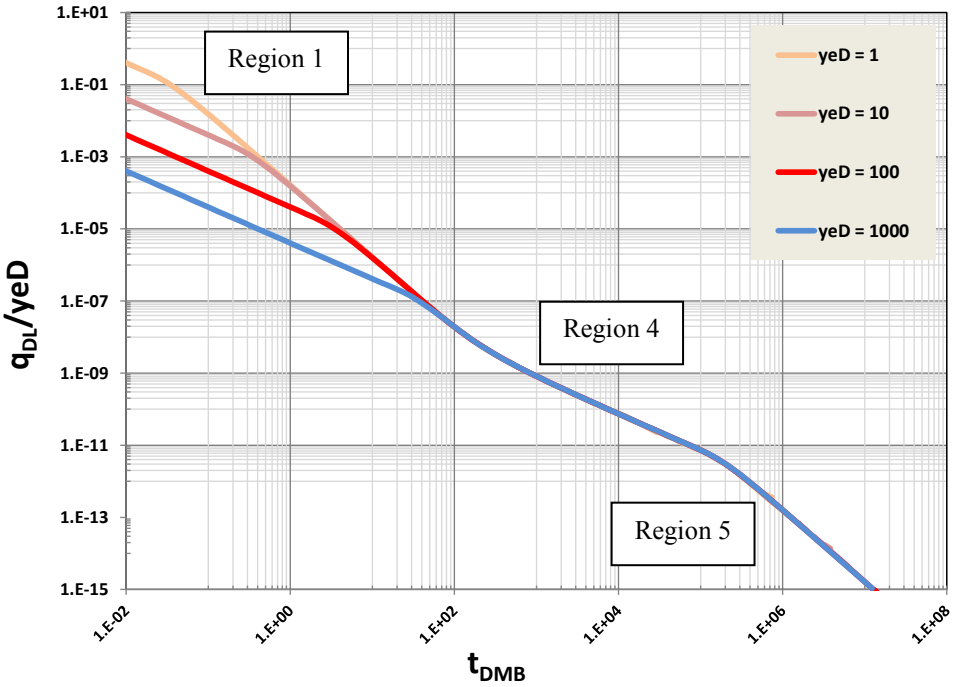

Fig. 5.6—Illustration of normalizing the effect of dimensionless fracture half-length by modifying the axis for a constant value of lambda and omega on log-log rate versus time plot

The final axis modification is to simplify the type curve for better and more accurate fitting and to use this modification for calculation which is going to be explained in details in later chapters. Fig. 5.7 shows the final type curve after modification. The Y-axis is modified by dividing the axis by the dimensionless fracture half-length (y_{eD}) and lambda (λ). The X-axis is modified by multiplying the axis by lambda (λ) only. Other modification were considered and illustrated with advantages and disadvantages on Appendix B.

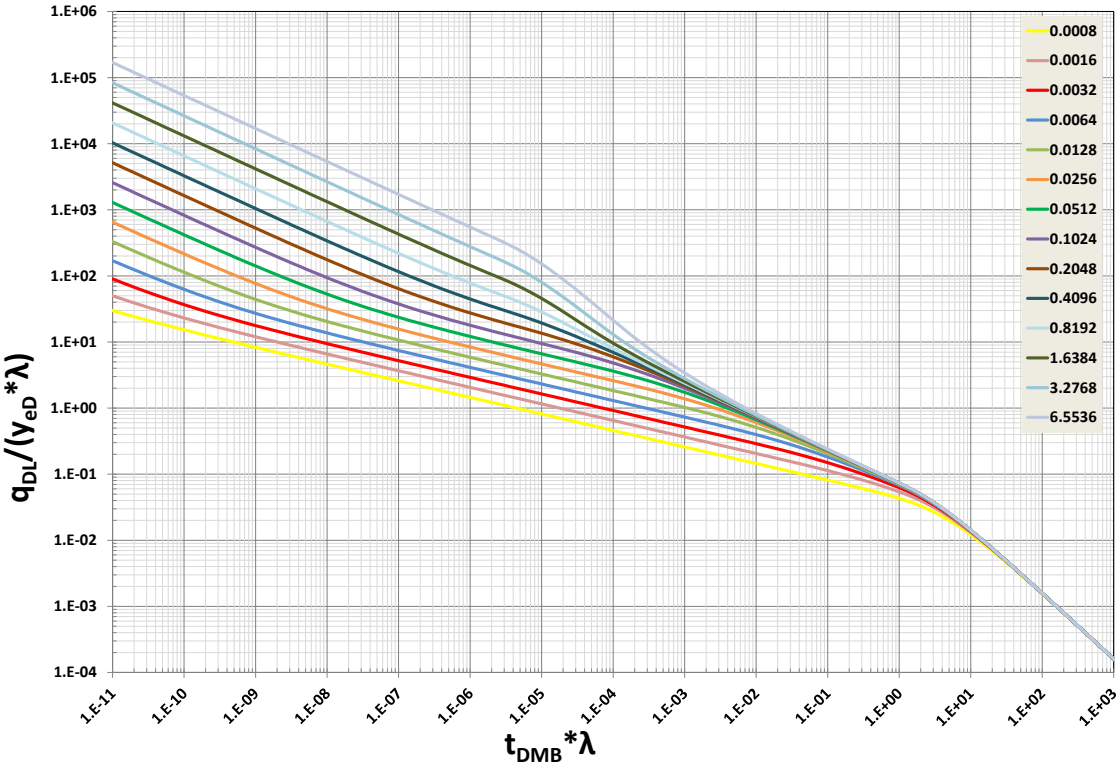

Fig. 5.7—Final type curve for linear dual porosity model after axis modification illustrated on log-log rate versus time plot

5.4.3 Other Specialized Plots

Curve fitting on a log-log plot can be bias. Visually, it looks like a good fit but in reality it needs a little correction. This is why it is important to fit more than one plot to insure an accurate answer. Other special type curve plots where made for this purpose such as derivative with natural logarithm of time plot and square root of time plots. Figs. 5.8, 5.9 and 5.10 illustrate some of these plots with the same axis modification.

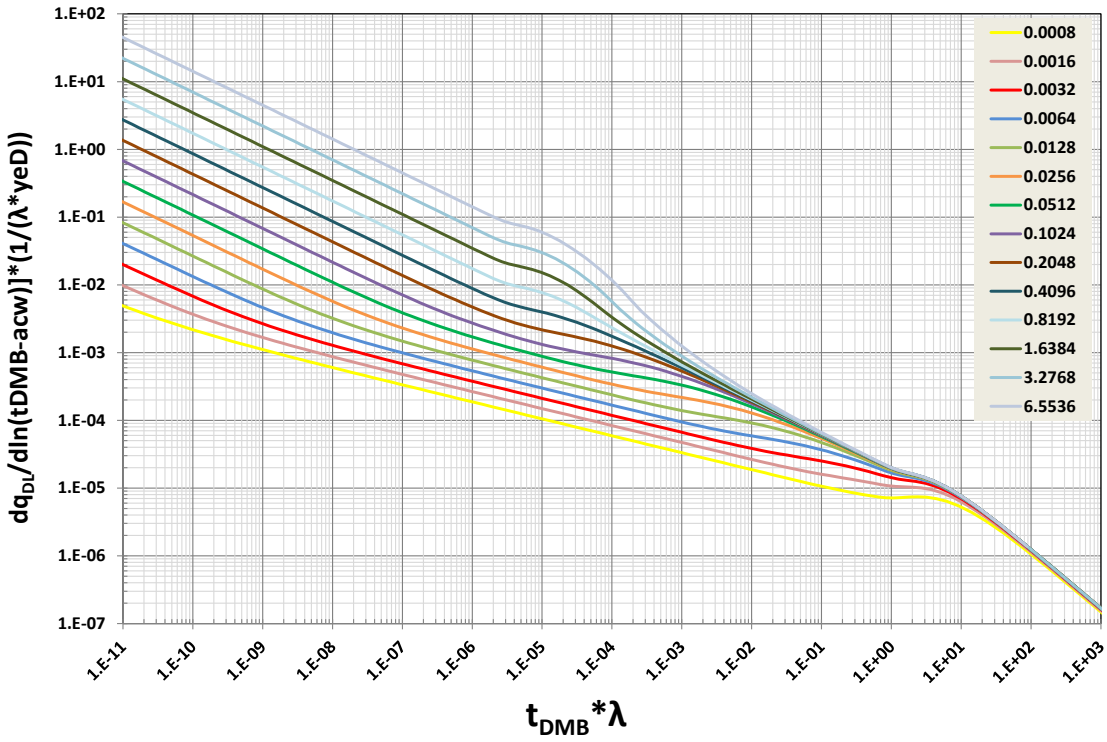

Fig. 5.8—Derivative with natural logarithm of material balance time for the final type curves for linear dual porosity model after axis modification

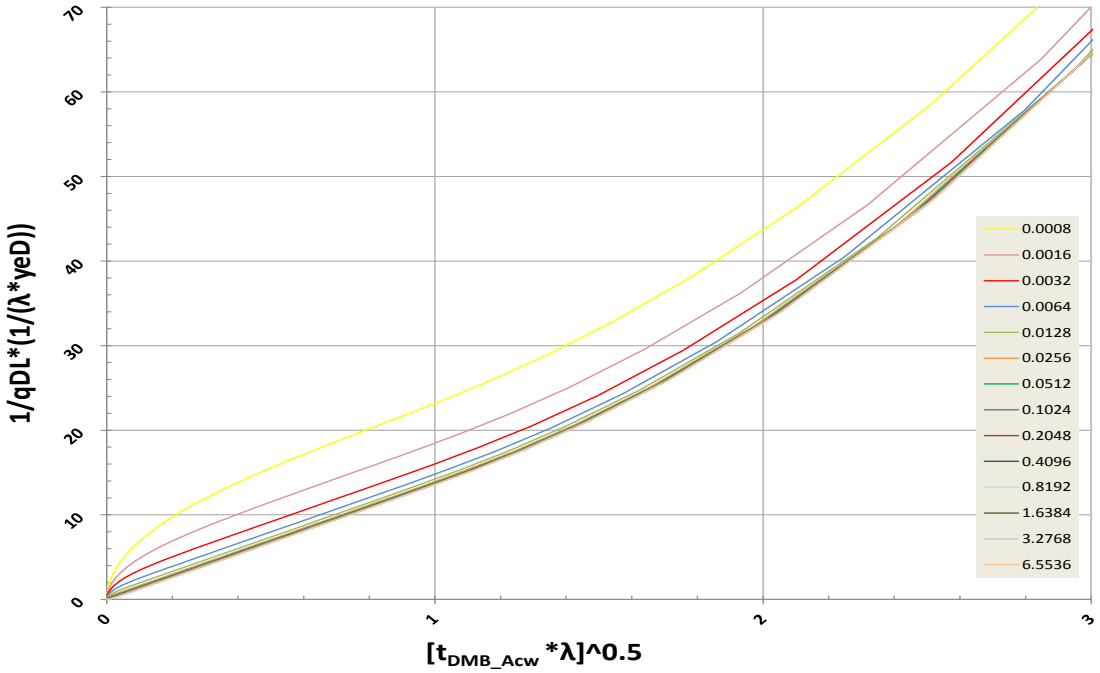

Fig. 5.9—Square root of material balance time for the final type curves for linear dual porosity model after axis modification

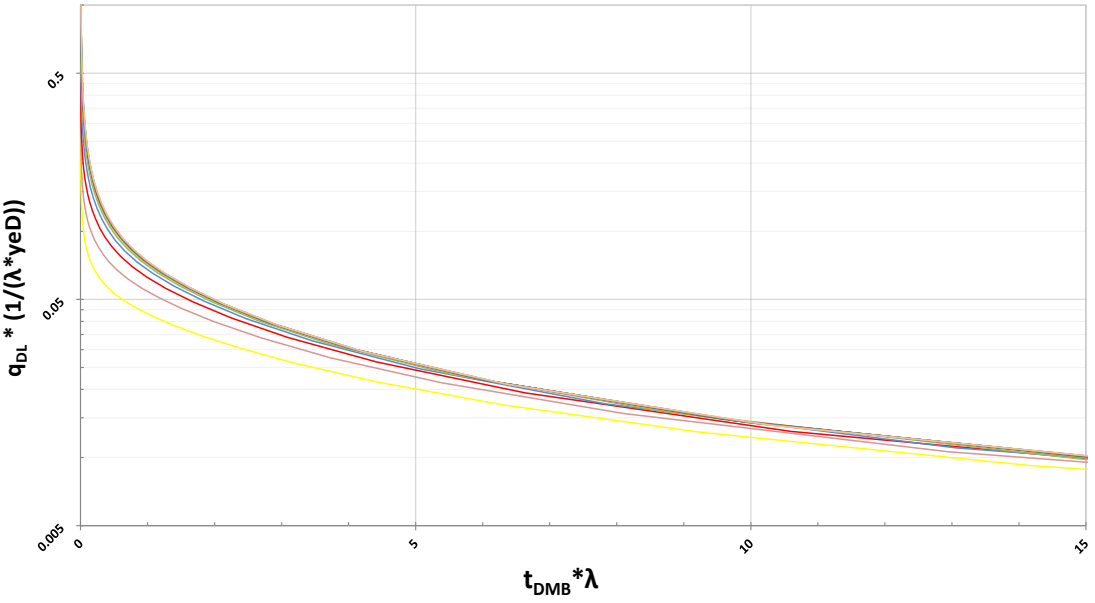

Fig. 5.10—Semi-log plot of the final type curves for linear dual porosity model after axis modification

5.4.4 Matching Points

To get a matching data, the normalized rate and its derivative with natural logarithm of material balance time should be plotted against the material balance time. After getting a good match, the rate shift and time shift should calculated. The match point for the dual porosity type curves are given as follows

$$\text{Rate Shift: } \frac{\left[q_{DL}\dfrac{1}{\lambda\, y_{eDAcw}}\right]_{M.P.}}{\left[\dfrac{q_g}{[m(p_i)-m(p)]}\right]_{M.P.}} = \frac{1}{\lambda\, y_{eDAcw}}\frac{1422T}{k_{eff}\sqrt{A_{cw}}} \quad \text{..... (5.9)}$$

$$\text{Time Shift: } \frac{\left[t_{D_{MB},A_{cw}}\,\lambda\right]_{M.P.}}{\left[t_{MB}\right]_{M.P.}} = \lambda\,\frac{0.00633k_{eff}}{\mu\phi_{eff}\,c_t\,A_{cw}} \quad \text{..... (5.10)}$$

These equations are going to be used to calculate the dual porosity parameters after curve fitting. Refer to Appendix A.

5.4.4 Calculation of Dual Porosity Parameters

Fig. 5.11 shows the calculation of dual porosity parameters flow chart. After getting a good fit on the dual porosity type curve, the inner effective fracture permeability is obtained. Using this value, the inter-porosity parameter (λ) is calculated. Using these calculated values, the dimensionless fracture half-length will be calculated using the matching point equations. Finally, the fracture half-length is going to be calculated using the definition of (y_{eD}).

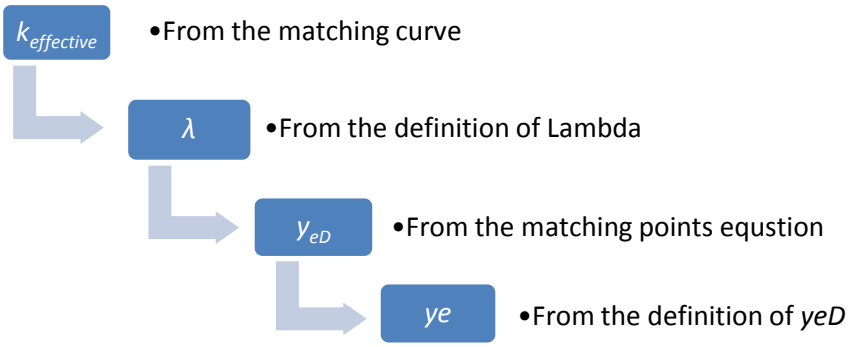

Fig. 5.11—Calculation of dual porosity parameters flow chart

5.5 Chapter Summary

In this chapter, the importance of the dual porosity effective parameters is shown. A new dual porosity parameters modification and assumption were proposed. A new type curve for linear dual porosity model is illustrated with its field cases coverage, axis modification, derivation, match points, and calculation.

CHAPTER VI

TYPE CURVE VALIDATION AND EXAMPLES

6.1 Introduction

In this chapter, the new type curves for linear dual porosity reservoir will be tested and validated against synthetic examples created by GASSIM which a single phase simulator and the commercial package CMG. Then, it will be tested against field example for shale gas. A VBA program will be viewed briefly which will be used to do all the matching cases.

6.2 Type Curve Matching VBA Program

A type curve matching program was created for a faster matching process using Visual Basic for Application (VBA) in Microsoft Excel. It will be also used to correct for the gas properties and calculate the *OGIP*, *EUR*, and *RF*. Fig. 6.1 shows the interface of type curve matching program.

A modified data smoothing method was adapted from (Bourdet 1989) and implemented in the program taken in consideration the beginning and end effect. Following is the algorithm used for the derivative

$$\left(\frac{dX}{dp}\right)_i = \frac{\Delta X_1 + \Delta X_2}{\left(\frac{\Delta X_1}{\Delta P_1}\right)\Delta X_2 + \left(\frac{\Delta X_2}{\Delta P_2}\right)\Delta X_1} \quad \text{..... (6.1)}$$

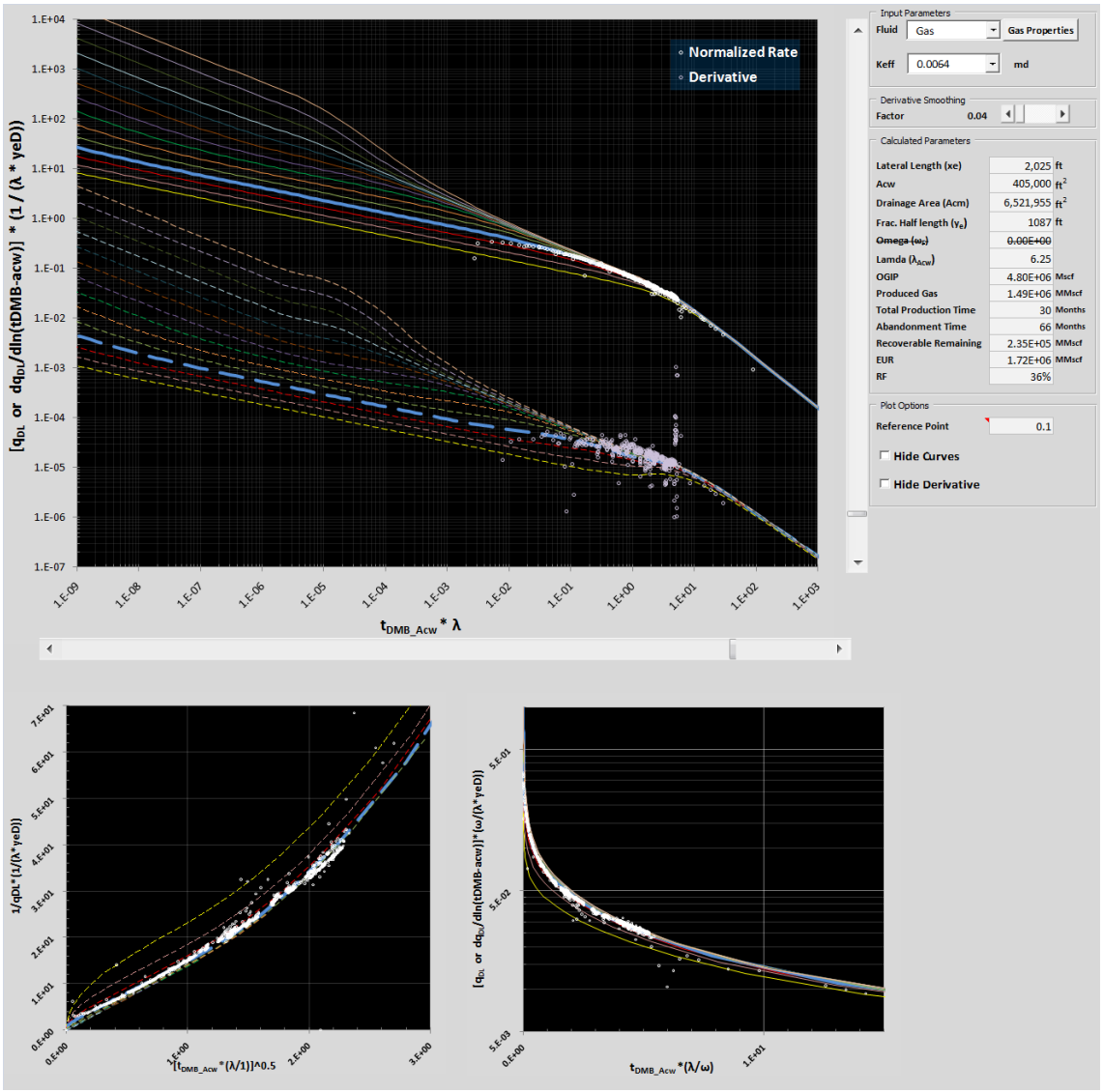

Fig. 6.1—Snapshot of the type curve matching program

6.3 Synthetic Cases

The data for the synthetic cases were generated using two programs, GASSIM which is a single phase simulator and Stehfest VBA which is an analytical simulator. Fig. 6.2 shows the example generated using Stehfest for random data to test how

accuracy of the shape of the curves. The case has a perfect match with curves. This is not a surprise since the same simulator was used to generate these set of curves.

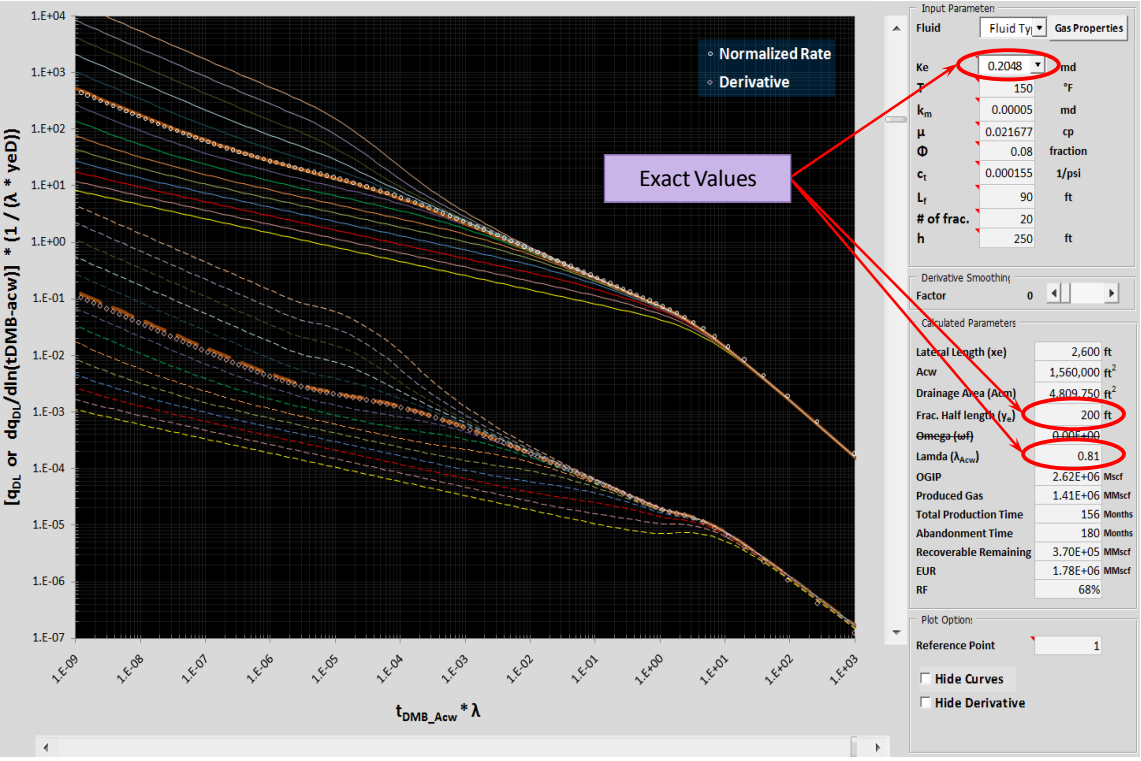

Fig. 6.2—Synthetic case generated with Stehfest to test the accuracy of the type curve shape

6.4 Synthetic Cases with Field History Matching

Several cases were generated using CMG commercial package for the purpose of validation. The data from a field well where loading into CMG with history matching. Then, this data was loaded into the type curve matching program for result comparison. The results from the type curves were closed to the data obtained from the simulator. Fig. 6.3 shows a well with boundary dominated flow. We have a good match on the

normalized rate curves. However, the derivative is matching with a high smoothing factor.

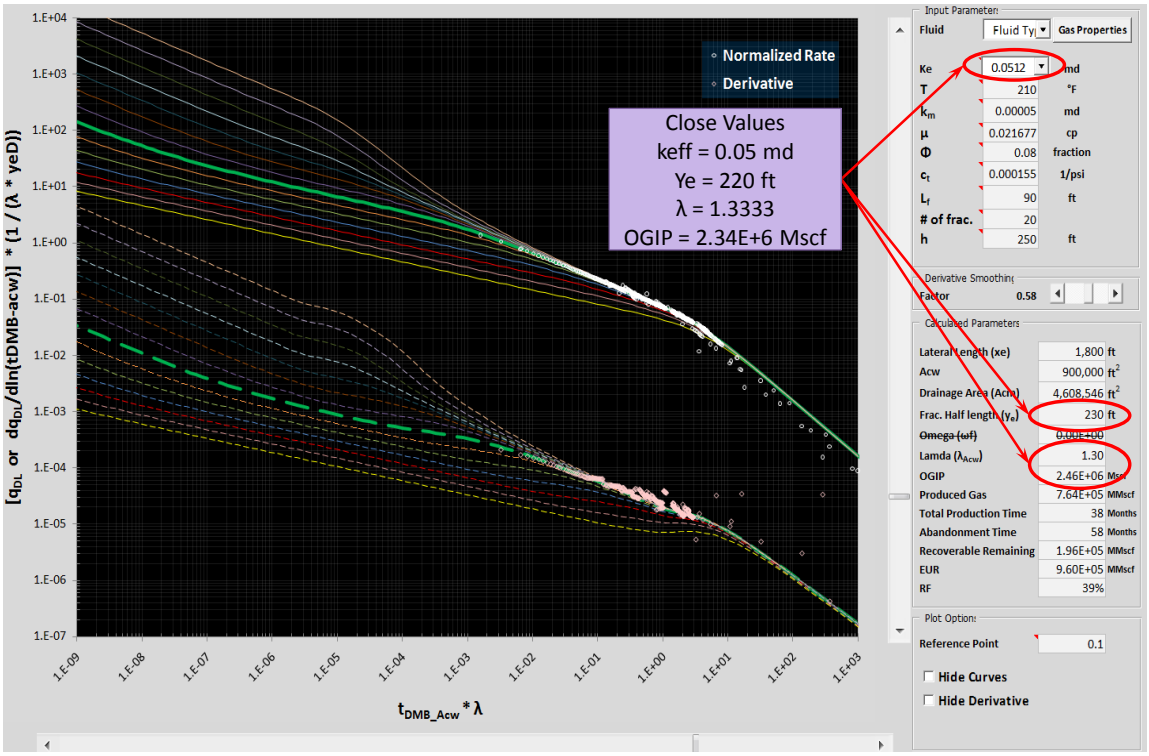

Fig. 6.3—Synthetic case generated with CMG to test the accuracy of type curve results which show very close values

Fig. 6.4 shows another synthetic example generated using CMG. This example shows a very good match for both the normalized rate and derivative. The calculated fracture half-length is considered a perfect match. Note that the smoothing factor for the derivative is very low comparing to the first example.

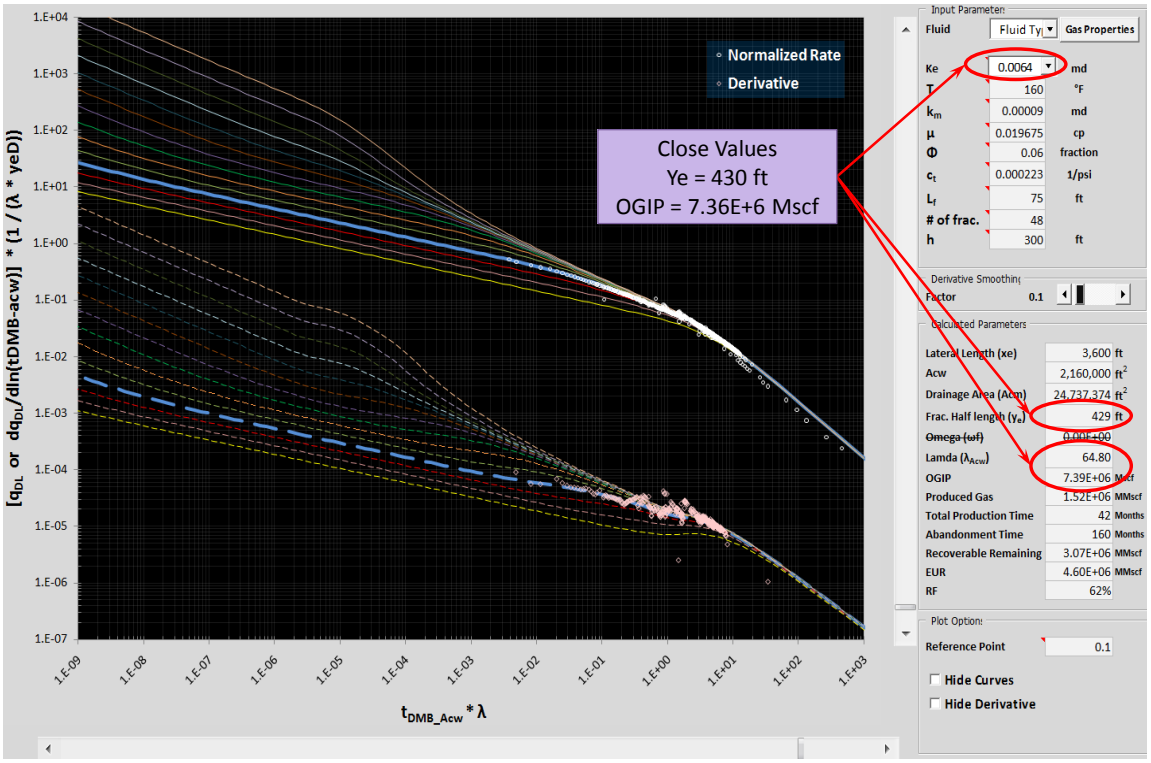

Fig. 6.4—Synthetic case generated with CMG to test the accuracy of type curve results show very close values

6.5 Field Cases

Several cases were run for shale gas wells. Some of these example results were compared to (Bello and Wattenbarger 2010) method using the same model. Two more plots were added to these runs to insure more accurate curve match.

The first example is well#314 from Barnett Shale. This well had been producing for almost three years. It has a very good clear half-slope and boundary dominated flow. Fig. 6.5 shows a very good match not only with normalized rate curve but also with square root time curves. The fracture half-length calculated is closed to the number calculated using (Bello and Wattenbarger 2010) method.

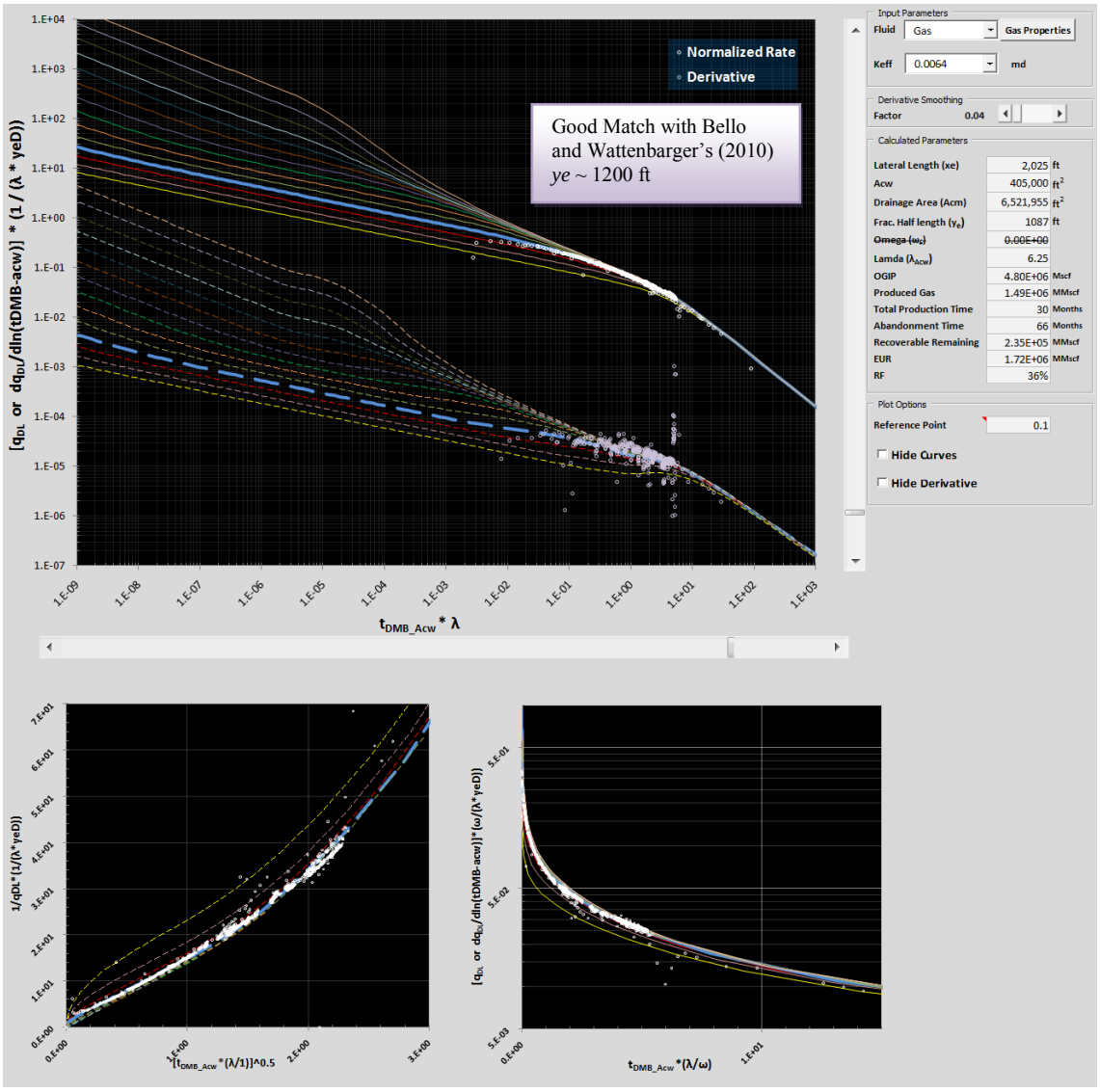

Fig. 6.5—Barnett Shale well # 314 shows a very good fit and results are close to those obtained from (Bello and Wattenbarger 2010) method

The second example is from Woodford shale. This well had been producing for almost four and half years. It is a known fact for this well that it has an interference problem with the nearby wells. The well is affected by three new horizontal wells with multi-stage fracture stimulation. Fig 6.6 shows a very good fit to the type curves.

Nevertheless, when looking closely at the data, the fit looks artificial. The production data is overlapping in different time intervals because of the bias of material balance time. More than one trend can be seen on the plot. This happens when the well gas rate drops and water production increases due to fracture treatment of nearby wells.

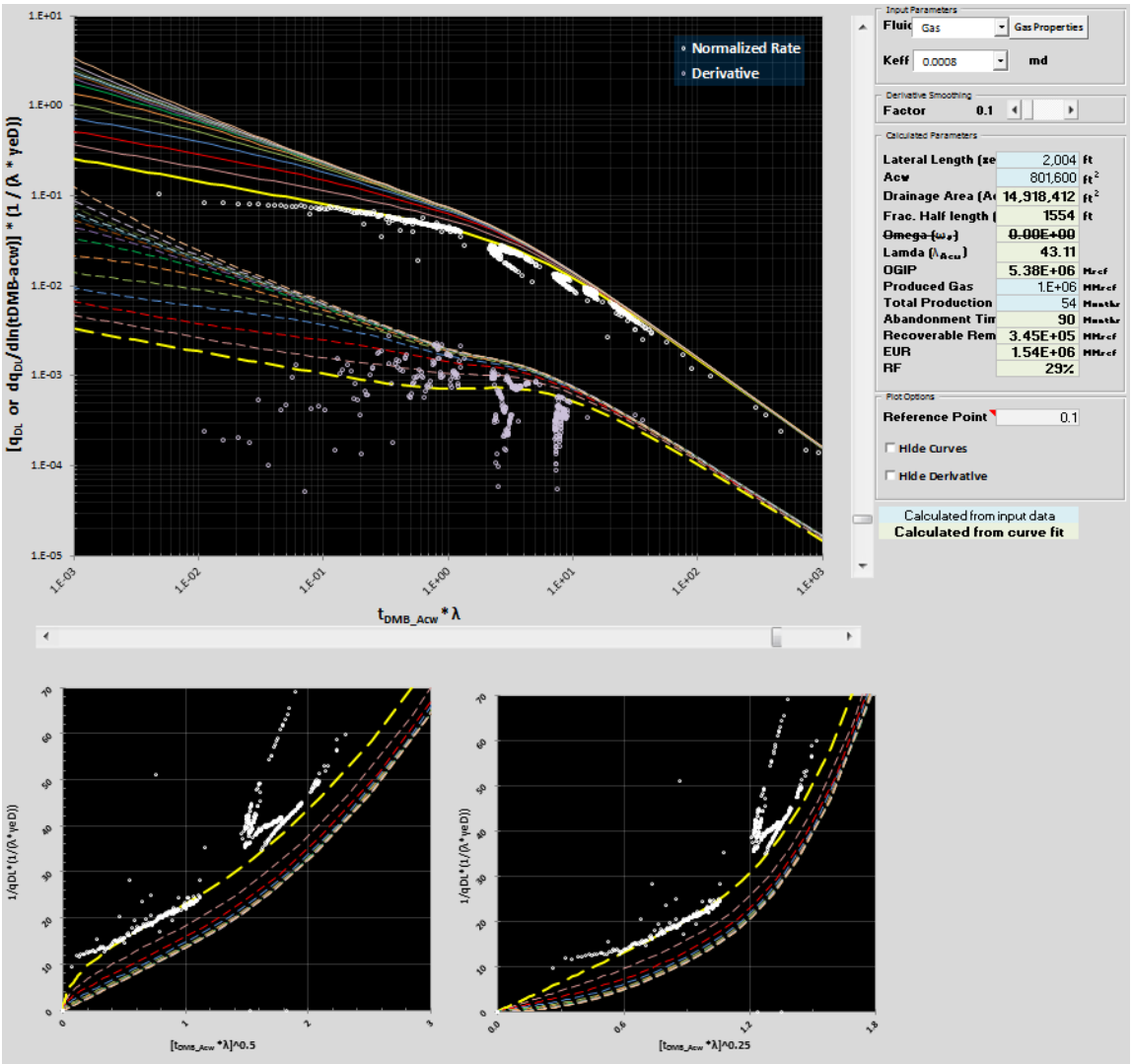

Fig. 6.6—Woodford shale well data shows the bias of material balance time

6.6 Results Discussion

A few examples were illustrated to show the power of this tool to calculate the unknown variable of the dual porosity reservoirs. The results show a very good accuracy for both synthetic and field data. However, there are few limitations to this method which can be true to any type curve analysis method. One of the drawbacks of this method is its dependency on the boundary dominated flow. The well has to see the boundary in order have an idea of what region of flow to match. A new well will be very difficult to match and may give a misleading answer. Another limitation appears with lack of data. If the well does not have enough data to match it will not give a unique match for the case. Another problem with data happens because of human intervention such as manipulating the flow from the surface. It can give wrong indications. Another limitation appears with the well interference that can create false signature and give a bad results even with a good match. To overcome this limitation a multi-well type curve analysis can be generated. Finally, the material balance time can create an artificial boundary dominated decline. In this case, the data will have a change in the slope because of the production rate change. The data should be examined on a regular performance plot before applying this method to avoid matching a wrong signature.

CHAPTER VII

CONCLUSIONS AND RECOMMENDATIONS

7.1 Conclusions

In this work a new method was proposed to analyze production performance of shale gas/oil wells using type curves. This method is based on linear flow equations in dual porosity reservoirs which were initially proposed by (El-Banbi 1998). Following are the main conclusions drawn from this research.

- The dual porosity parameters were analyzed and their effect of the shape of the well production was observed.
- The physical dual porosity parameters were analyzed and their effect of the shape of the well production was observed.
- New effective parameters for the dual porosity linear model were proposed to make it easier to generate type curve solutions.
- It was found that some dual porosity parameters can be normalize by modifying the axis; namely the dimensionless fracture half-length (y_{eD})
- New type curves were developed to match production performance of shale gas/oil wells with linear Dual Porosity model.
- Software was developed in Excel's VBA to implement the proposed type curve.

- Different synthetic cases were checked on Software to prove accuracy of proposed type curves.
- The type curves were applied to field examples. Excellent matches were obtained with field data.
- It was proved that the type curve proposed proposed in this work is an accurate and robust tool to analyze the production of shale gas/oil well in short period of time.

7.2 Recommendations for Future Work

- More work should be done to include the influence of the effective porosities on these type curves.
- More work should be done to be able to calculate more accurate values of the storativity ratio (omega).
- Type Curves can be generated to match production of shale gas/oil wells with triple Porosity model.
- Multi-well type curve analysis can be added to this work.

NOMENCLATURE

A_{cw} = cross sectional area to the flow, ft^2

c_f = formation compressibility, 1/psi

c_g = gas compressibility, 1/psi

c_t = total compressibility, 1/psi

c_w = water compressibility, 1/psi

k_F = effective fracture permeability, md

$k_{effective}$ = inner effective fracture permeability, md

k_m = matrix permeability, md

L_F = Fracture Spacing, ft

$m(p_i)$ = pseudo initial pressure, psi^2/cp

$m(p_{wf})$ = pseudo bottom hole flowing pressure, psi^2/cp

$OGIP$ = original gas in place, Bscf

p = pressure, psi

$\bar{p}$ = average pressure, psi

q_{DL} = dimensionless rate

q_g = gas rate, Mscf/Day

S_{wi} = initial water saturation

SRV = stimulated reservoir volume

$t_{DA_{cw}}$ = dimensionless time

t_{DMB} = dimensionless material balance time

T = temperature, degrees R

x_e = perforated well length, ft

y_e = fracture half length, ft

y_{eD} = dimensionless fracture half length

Greek Symbols

μ_g = gas viscosity, cp

φ = porosity

λ = inter-porosity coefficient

ω = storativity coefficient

ω' = modified storativity coefficient

REFERENCES

Ahmadi, H. A. A., Almarzooq, A. M., and Wattenbarger, R. A. 2010. Application of Linear Flow Analysis to Shale Gas Wells: Field Cases. Paper SPE 130370 presented at the Unconventional Gas Conference, Pittsburgh, Pennsylvania, USA. 23-25 February.

Arevalo-Villagran, J. A., Wattenbarger, R. A., Samaniego-Verduzco, F., Pham, Tai T. 2001. Production Analysis of Long-Term Linear Flow in Tight Gas Reservoirs: Case Histories. Paper SPE 71516 presented at the Annual Technical Conference and Exhibition, New Orleans, Louisiana. 30 September-3 October.

Bello, R. O. and Wattenbarger, R. A. 2008. Rate Transient Analysis in Naturally Fractured Shale Gas Reservoirs. Paper CIPC/SPE 114591 presented at the Gas Technology Symposium 2008 Joint Conference, Calgary, Alberta, Canada. 16-19 June.

Bello, R. O. and Wattenbarger, R. A. 2009. Modelling and Analysis of Shale Gas Production with a Skin Effect. Paper CIPC 2009-082 presented at the Canadian International Petroleum Conference, Calgary, Alberta. 16 - 18 June.

Bello, R. O. and Wattenbarger, R. A. 2010. Multi-Stage Hydraulically Fractured Horizontal Shale Gas Well Rate Transient Analysis. Paper SPE 126754 presented at the North Africa Technical Conference and Exhibition, Cairo, Egypt. 14-17 February.

Bourdet, D., Ayoub, J. A., and Pirard, Y. M. 1989. Use of Pressure Derivative in Well Test Interpretation. SPE Formation Evaluation (June): 293-302. SPE-12777-PA

Da Prat, G., Cinco-Ley, H., and Ramey Jr., H. 1981. Decline Curve Analysis Using Type Curves for Two-Porosity Systems. SPE J. (June): 354-362. SPE-9292-PA

de Swaan O., A. 1976. Analytic Solutions for Determining Naturally Fractured Reservoir Properties by Well Testing. SPE J. (June): 117-122. SPE-5346-PA.

El-Banbi, A., H. and Wattenbarger, R. A. 1998. Analysis of Linear Flow in Gas Well Production. Paper SPE 39972 presented at the Gas Technology Symposium, Calgary, Alberta, Canada. 15-18 March.

El-Banbi, A. H. 1998. Analysis of Tight Gas Well Performance. Doctor of Philosophy, Texas A&M University, College Station, Texas.

Hazlett, W. G., Lee, W. J., Narahara, G. M., Gatens III, J. M. 1986. Production Data Analysis Type Curves for the Devonian Shales. Paper SPE 15934 presented at the Eastern Regional Meeting, Columbus. Ohio. 12-14 November.

Kazemi, H. 1969. Pressure Transient Analysis of Naturally Fractured Reservoirs with Uniform Fracture Distribution. SPE J. (December):451– 462. SPE-2156A-PA.

Moghadam, S., Mattar, L., and Pooladi-Darvish, M. 2010. Dual Porosity Typecurves for Shale Gas Reservoirs. Paper SPE 137535 presented at the Canadian Unconventional Resources and International Petroleum Conference, Calgary, Alberta, Canada. 19-21 October.

Palacio, J. C. and Blasingame, T. A. 1993. Decline-Curve Analysis with Type Curves Analysis of Gas Well Production Data. Unpublished Preprint. Paper SPE 25909 presented at the Rocky Mountain Regional/Low Permeability Reservoirs Symposium, Denver, Colorado, USA. 12-14 April.

Samandarli, O., Ahmadi, H. A. A., and Wattenbarger, R. A. 2011. A New Method for History Matching and Forecasting Shale Gas Reservoir Production Performance with a Dual Porosity Model. Paper SPE 144335 presented at the North American Unconventional Gas Conference and Exhibition, The Woodlands, Texas, USA. 14-16 June.

van Everdingen, A. F. and Hurst, W. 1949. The Application of the Laplace Transformation to Flow Problems in Reservoirs. Petroleum Transactions, AIME (December): 305 – 324. SPE-949305-G

Warren, J. E. and Root, P. J. 1963. The Behavior of Naturally Fractured Reservoirs. Paper SPE 426-PA presented at the fall meeting of Society of Pertroleum Engineers, Los Angeles, California, USA. 7-10 October.

APPENDIX A

MATCH POINTS AND LINKING OF EFFECTIVE PARAMETERS FOR LINEAR DUAL POROSITY MODEL

Dimensionless Variables

$$t_{DA_{cw}} = \frac{0.00633 k_F t}{\phi \mu c_t A_{cw}} \quad \text{.....(A-1)}$$

$$\frac{1}{q_{DL}} = \frac{k_F \sqrt{A_{cw}} \left[m(p_i) - m(p_{wf}) \right]}{1422 q_g T} \quad \text{.....(A-2)}$$

$$\frac{1}{q_{DL}} = \frac{k_F \sqrt{A_{cw}} \left[p_i - p_{wf} \right]}{141.2 q_o B \mu} \quad \text{.....(A-3)}$$

$$\lambda = \frac{12}{L_F^2} \frac{k_m}{k_F} A_{cw} \quad \text{.....(A-4)}$$

$$\omega = \frac{\left[\phi V c_t \right]_F}{\left[\phi V c_t \right]_t} \quad \text{.....(A-5)}$$

$$y_{eD} = \frac{y_e}{\sqrt{A_{cw}}} \quad \text{.....(A-6)}$$

$$k_{effective} = \frac{k_m L_F + k_F w_F}{L_F + w_F} \quad \text{.....(A-7)}$$

Linking the effective parameters

Fracture and matrix bulk volume for model one,

$$V_{bF} = \frac{w_F}{2} 4n \; y_e h \quad \text{.....(A-8)}$$

$$V_{bm} = \frac{L_F}{2} 4n\ y_e h \quad \text{.....(A-9)}$$

Fracture and matrix bulk volumes by taking the ratio for Eq. A-8 and A-9,

$$V_F = \frac{V_{bF}}{V_{bt}} = \frac{w_F}{w_F + L_F} \quad \text{..... (A-10)}$$

$$V_m = \frac{V_{bm}}{V_{bt}} = \frac{L_F}{w_F + L_F} \quad \text{..... (A-11)}$$

Simplifying omega on Eq. A-5 by assuming $c_{tt} \approx c_{Ft}$,

$$\omega_F = \frac{[\phi V]_F}{[\phi V]_m + [\phi V]_F} \quad \text{..... (A-12)}$$

Substituting Eq. A-10 and Eq. A-11 on Eq. A-12,

$$\omega_F = \frac{\phi_F \left[\frac{w_F}{w_F + L_F} \right]}{\phi_m \left[\frac{L_F}{w_F + L_F} \right] + \phi_f \left[\frac{w_F}{w_F + L_F} \right]} \quad \text{..... (A-13)}$$

Eq. A-12 is simplified,

$$\omega_F = \frac{w_F \phi_F}{w_F \phi_F + L_F \phi_m} \quad \text{..... (A-14)}$$

Another form of Eq. A-13,

$$\omega_F = \frac{\phi_F}{\phi_F + \frac{L_F}{w_F} \phi_m} \quad \text{..... (A-15)}$$

Solving for L_F/w_F in Eq. A-7,

$$\frac{L_F}{w_F} = \frac{\left[1 - \frac{k_F}{k_{effective}}\right]}{\left[\frac{k_m}{k_{effective}} - 1\right]} \quad \text{..... (A-16)}$$

Substituting Eq. A-16 in Eq. A-15,

$$\omega_F = \frac{\phi_F}{\phi_F + \frac{\left[1 - \frac{k_F}{k_{effective}}\right]}{\left[\frac{k_m}{k_{effective}} - 1\right]}\phi_m} \quad \text{..... (A-17)}$$

Rearranging the equation,

$$\omega_F = \frac{1}{1 + \frac{\phi_m}{\phi_F}\left[\frac{(k_{effective} - k_F)}{(k_m - k_{effective})}\right]} \quad \text{..... (A-18)}$$

Match Point Equations

Rate Shift:

Multiply Eq. A-2 by the shifting factor (1/yeD*λ),

$$\left[q_{DL}\frac{1}{\lambda\, y_{eDAcw}}\right]_{M.P.} = \frac{1}{\lambda\, y_{eDAcw}}\frac{1422T}{k_{eff}\sqrt{A_{cw}}}\left[\frac{q_g}{[m(p_i) - m(p)]}\right]_{M.P.} \quad \text{..... (A-19)}$$

Rearrange the Eq. A-19,

$$\frac{\left[q_{DL}\,\frac{1}{\lambda\, y_{eDAcw}}\right]_{M.P.}}{\left[\frac{q_g}{[m(p_i)-m(p)]}\right]_{M.P.}} = \frac{1}{\lambda\, y_{eDAcw}}\,\frac{1422T}{k_{eff}\sqrt{A_{cw}}} \quad \text{..... (A-20)}$$

Time Shift:

Multiply Eq. A-1 by the shifting factor (λ),

$$\left[t_{D_{MB},A_{cw}}\,\lambda\right]_{M.P.} = \lambda\,\frac{0.00633k_{eff}}{\mu\phi_{eff}\,c_t\,A_{cw}}\left[t_{MB}\right]_{M.P.} \quad \text{..... (A-21)}$$

Rearrange the Eq. A-21,

$$\frac{\left[t_{D_{MB},A_{cw}}\,\lambda\right]_{M.P.}}{\left[t_{MB}\right]_{M.P.}} = \lambda\,\frac{0.00633k_{eff}}{\mu\phi_{eff}\,c_t\,A_{cw}} \quad \text{..... (A-22)}$$

APPENDIX B

OTHER TYPE CURVES DEVELOPED FOR DUAL POROSITY LINEAR SYSTEM

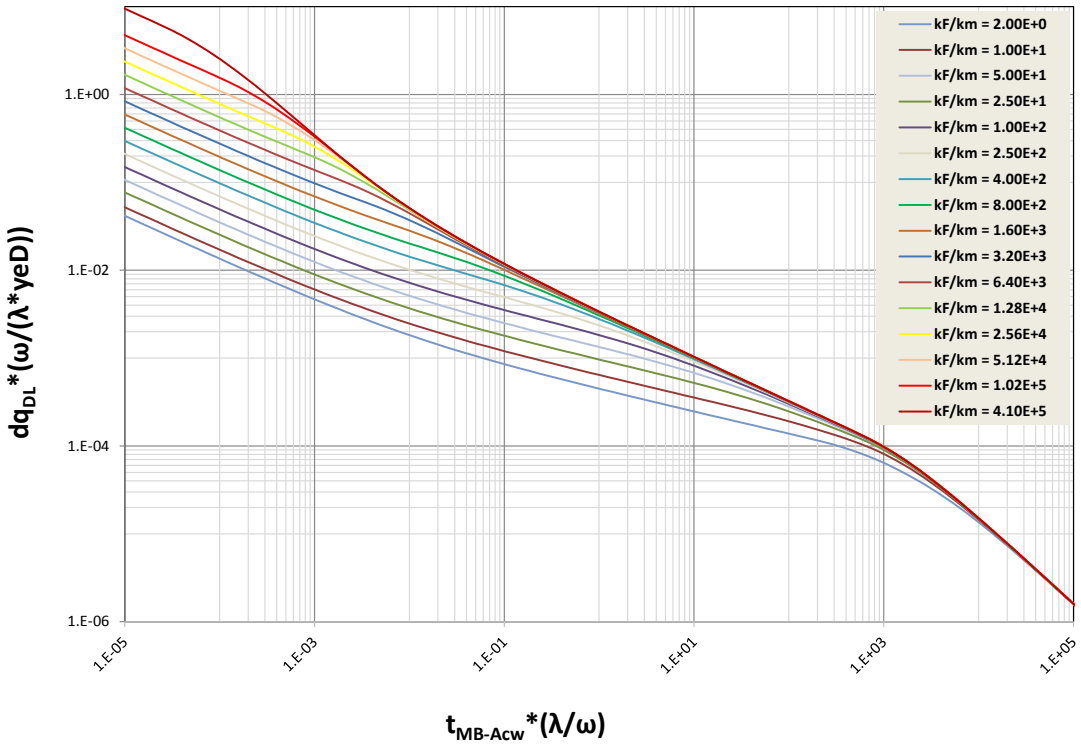

Fig. (B-1)—Type curve generated using the ratio of the effective permeability to the matrix permeability

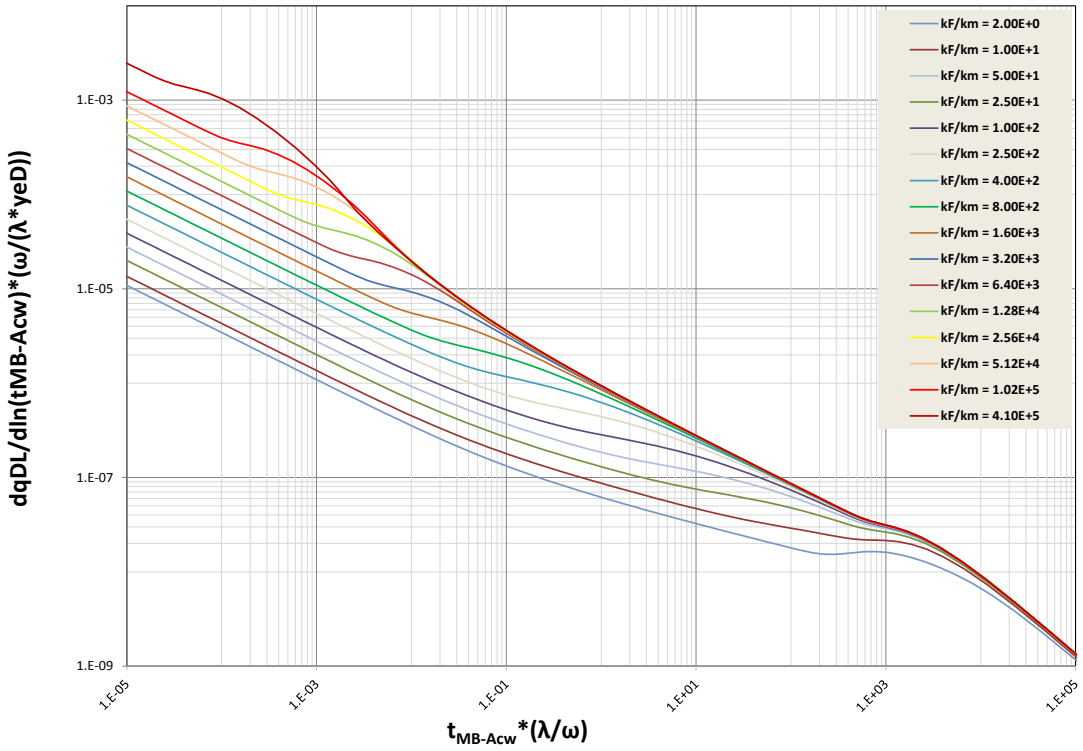

Fig. (B-2)—Derivative of type curve generated using the ratio of the effective permeability to the matrix permeability

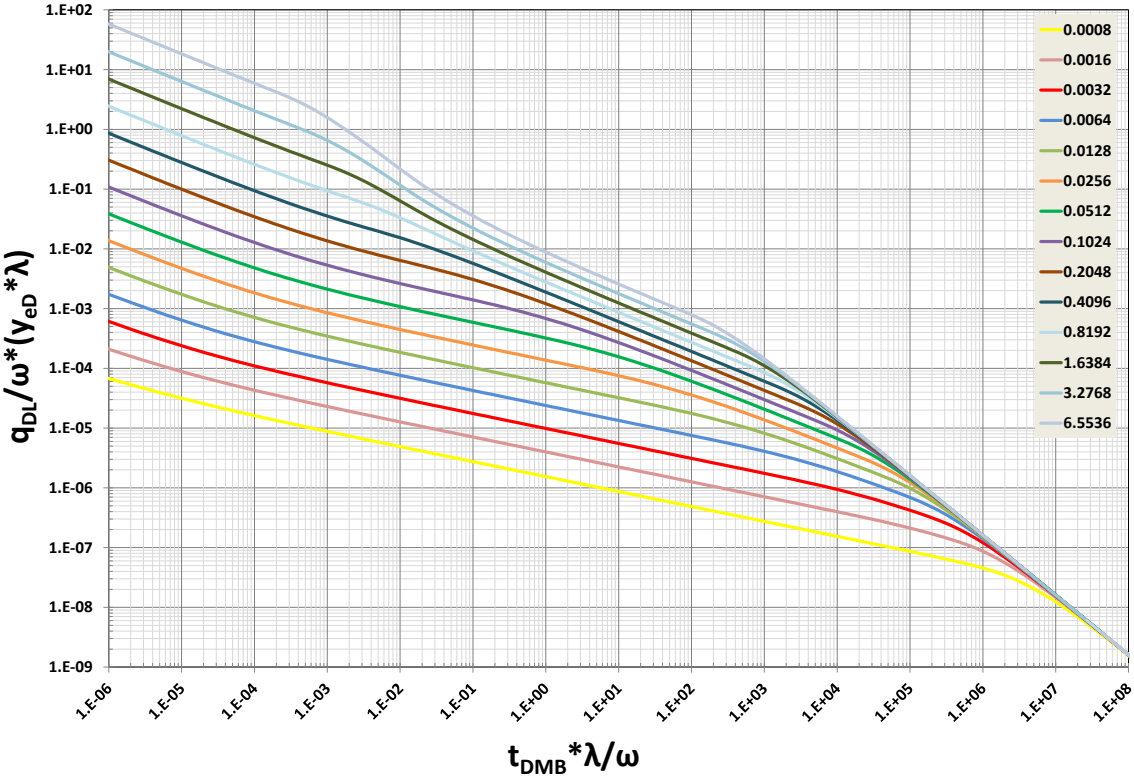

Fig. (B-3)—Type curve generated using the inner effective permeability but for different axis modification using omega as a factor

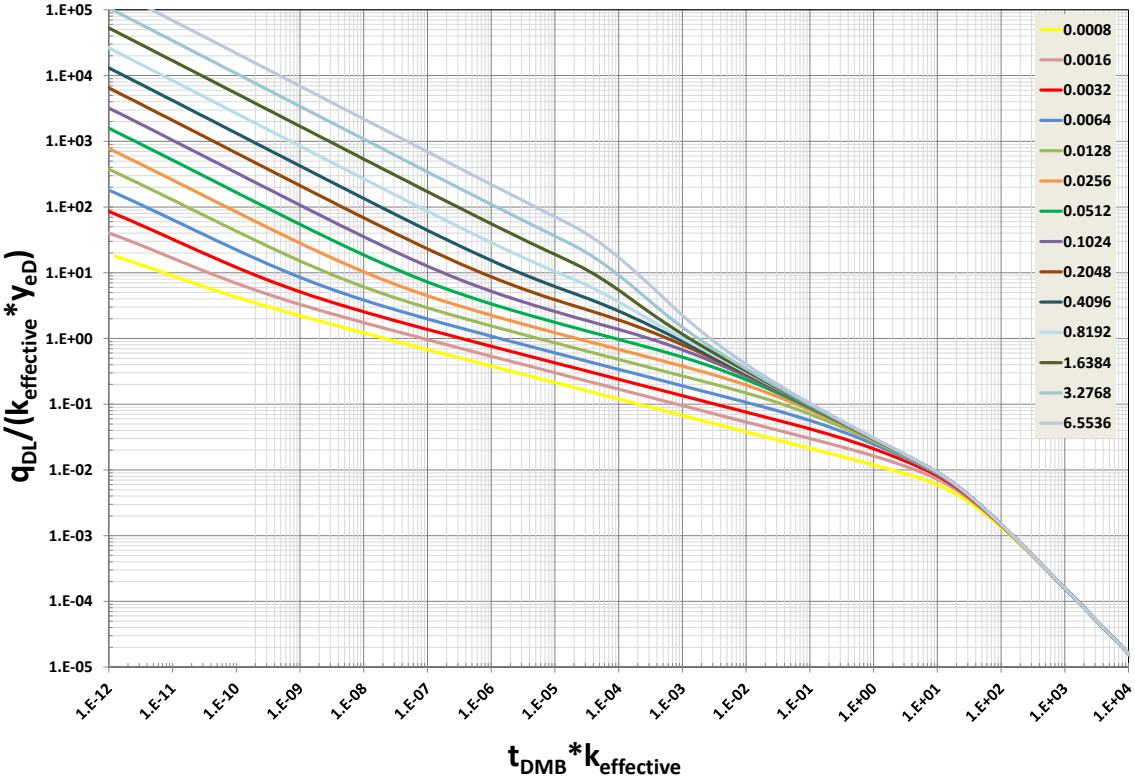

Fig. (B-4)—Type curve generated using the inner effective permeability but for different axis modification using effective permeability as a factor

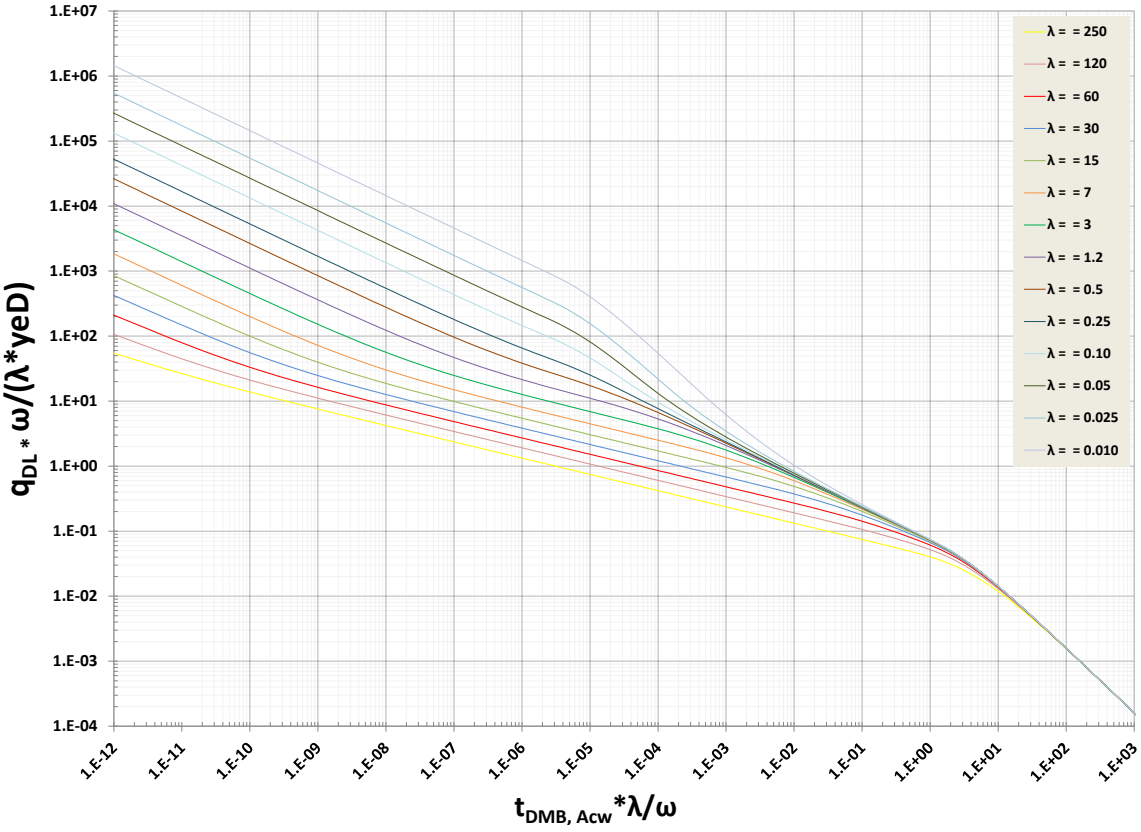

Fig. (B-5)—Type curve generated using the inter-porosity parameter lambda but for different axis modification using omega as a factor

VITA

Name: Haider Jaffar Abdulal

Address: Harold Vance Department of Petroleum Engineering
Texas A&M University
3116 TAMU - 507 Richardson Building
College Station, TX 77843-3116

Email Address: abdulahj@aramco.com

Education: B.S., Petroleum Engineering, University of Tulsa
Tulsa, Oklahoma, USA, 2005

M.S., Petroleum Engineering, Texas A&M University,
College Station, USA, 2011